

IONIZATION OF AIR BY
CORONA DISCHARGE

The members of the Committee approve the master's
thesis of Philip Koshy Panicker

Frank K. Lu
Supervising Professor

George Emanuel

Bernard T. Svihel

Copyright © by Philip K. Panicker 2003

All Rights Reserved

IONIZATION OF AIR BY
CORONA DISCHARGE

by

PHILIP KOSHY PANICKER

Presented to the Faculty of the Graduate School of
The University of Texas at Arlington in Partial Fulfilment
of the Requirements
for the Degree of

MASTER OF SCIENCE IN AEROSPACE ENGINEERING

THE UNIVERSITY OF TEXAS AT ARLINGTON

August 2003

ACKNOWLEDGEMENTS

I wish to thank Dr. Frank Lu, Director of the Aerospace Research Centre (ARC) and Dr. Don Wilson, Chairman of the Mechanical and Aerospace Engineering Department (MAE), for the opportunity to work at the ARC and for giving me the Graduate Teaching Assistantship for the period of my research. I would like to thank my advisors Dr. Lu, Dr. George Emanuel (MAE) and Dr. Bernard T. Svihel (Electrical Engineering Department) for their guidance and direction. This project was funded by Dr. Emanuel and the Mechanical and Aerospace Engineering Department, for which I am very grateful. I would like to thank my project associate Satyanand Udhyavar for his partnership and support in the project. I would like to thank Dr. Wei-Jen Lee, of the Electrical Engineering Department, for his timely help with the electronic circuits. I would like to thank Rod Duke of the ARC for his services in manufacturing the hardware of the project and other technical help. I would like to thank my colleagues at the ARC, Jason Myers and Chris Roseberry, for their help. I would like to thank Rafaela Bellini for all her help and support.

I would like to thank my father Koshy Panicker, my mother Deenamma, my brother John and my sister Anu for their love, support and prayers.

I want to thank my Lord and saviour Jesus Christ for all His blessings in my life. May everything be for the glory of God.

July, 2003

ABSTRACT

IONIZATION OF AIR BY CORONA DISCHARGE

Publication No. _____

Philip K. Panicker, MS

The University of Texas at Arlington, 2003

Supervising Professor: Frank K. Lu

The objective of this project is to create low density plasma by generating corona discharge by applying a high dc potential in a test section, consisting of a steel tube with a wedge shaped electrode. Once ionization has been initiated, a probe is introduced into the plasma to detect plasma characteristics at various axial distances away from the test section. This is to measure how far away from the electrodes the plasma persists in the air. A high voltage dc power supply has been designed and assembled specifically for this project. This study is a precursor to an upcoming research study to ionize supersonic air in a shock tunnel by the same corona discharge method. Therefore the test section built for this study is designed to fit onto a shock tunnel. The high voltage dc power supply is also designed to be applied to the

supersonic corona discharge study. This study will help in the design of diagnostic probes and apparatus for the analysis of plasma created within the supersonic flow in the upcoming project. Results from this study show that corona discharge is taking place and it has been verified visually and by measurements of voltage and current and ions emanating into the ambient air from the test section have been detected. These results show that the test section, the power supply and other apparatus developed can be applied to the supersonic corona discharge study.

TABLE OF CONTENTS

ACKNOWLEDGEMENTS.....	iv
ABSTRACT	v
LIST OF ILLUSTRATIONS.....	xi
LIST OF TABLES.....	xiv
LIST OF ABBREVIATIONS AND SYMBOLS	xv
Chapter	
1. INTRODUCTION	1
1.1 Plasma studies in Aerospace Engineering.....	1
1.1.1 Previous Research	1
1.2 Previous Plasma Related Work at UT Arlington.....	2
1.3 Brief Description of This Project.....	4
1.3.1 Applications for this Study	6
1.3.2 Overview of the Experimental Setup.....	6
2. THE CORONA DISCHARGE PHENOMENON.....	8
2.1 Plasma	8
2.1.1 Properties of Plasma	10
2.2 Ionization of Air.....	11
2.2.1 Particle Impact Ionization.....	12

2.2.2 Thermal Ionization.....	12
2.2.3 Nuclear Emission.....	13
2.2.4 Photo or Irradiative Ionization.....	13
2.2.5 Electric Field Ionization	13
2.3 Corona Discharge.....	14
2.3.1 Features of Corona Discharge	15
2.3.2 Corona vs. Arcs and Sparks.....	19
2.3.3 Earlier Work Involving Corona Discharge.....	20
3. DESIGN OF THE HIGH VOLTAGE POWER SUPPLY.....	22
3.1 Requirements of the Power Supply.....	22
3.2 Types of High Voltage Generators	23
3.2.1 Voltage Multipliers.....	24
3.2.2 Van de Graaff Generator	25
3.2.3 Tesla Coil.....	25
3.2.4 Step-Up Transformer and Rectifier Power Supply.....	26
3.2.4.1 Fly Back Transformer or Line Output Transformer	26
3.2.4.2 Microwave Oven Power Supply	28
3.2.4.3 Ignition Transformers	29
3.2.4.4 Neon Transformer	29
3.3 The Neon Transformer.....	31
3.3.1 Normal Power Transformer Operation.....	32
3.3.2 Power Factor.....	33

3.3.3 Features.....	34
3.4 The Autotransformer.....	36
3.5 The Diodes.....	38
3.6 The Capacitor.....	44
3.7 The Power Relays.....	45
3.7.1 Electromechanical Relays vs. Solid State Switches	47
3.7.2 Power Relays Used in the Circuit.....	48
3.8 DC Voltage Measurement.....	49
3.9 The Control Box.....	52
3.10 Features of the High Voltage Power Supply.....	54
3.10.1 Current Limiting and Capacitor Discharging Resistors.....	59
3.11 Current Measurement of the High Voltage DC Output.....	62
3.12 Safety Features of the High Voltage DC Power Supply.....	63
3.13 Drawbacks of the High Voltage DC Power Supply.....	64
3.14 Operation of the High Voltage DC Power Supply.....	65
4. THE CORONA DISCHARGE TEST SECTION	69
4.1 Features of the Design	69
4.1.1 Mechanical Aspects of this Design.....	70
4.1.2 Electrical Aspects of this Design.....	71
5. ION DETECTION PROBES.....	74
5.1 Langmuir Probes.....	76
5.2 Probes Used in the Bench Test	78

6. BENCH TESTING OF TEST SECTION IN STATIC AND SLOW SPEED AIR.....	81
6.1 Bench Test Results.....	81
6.2 Malter Effect.....	85
6.3 Results of the Ion Detector Probes.....	87
7. CONCLUSION AND RECOMMENDATIONS	89
7.1 Conclusion.....	89
7.2 Recommendations.....	90
Appendices	
A. CIRCUIT DIAGRAM OF THE HIGH VOLTAGE AC GENERATOR.....	92
B. CIRCUIT DIAGRAM OF THE HIGH VOLTAGE DC POWER SUPPLY	94
C. CIRCUIT DIAGRAM OF THE CONTROL BOX	96
REFERENCES	98
BIOGRAPHICAL INFORMATION.....	102

LIST OF ILLUSTRATIONS

Figure		Page
1.1	The Hypersonic Shock Tunnel of the ARC	3
1.2	Schematic of the Detonation Driven Shock Tube.....	3
1.3	Schematic of the Conventional Shock Tube	4
1.4	Schematic of the Experimental Setup	7
2.1	A Pulse Waveform	19
3.1	Voltage Multiplier Circuit.....	24
3.2	Schematic of the High Voltage DC Power Supply	30
3.3	Schematic of a Transformer	33
3.4	Current Lagging Voltage by 60°	34
3.5	Schematic of a Neon Transformer	35
3.6	The Circuit Diagram of an Autotransformer.....	36
3.7	Connection of the Autotransformer to the Neon Transformer.....	37
3.8	Single Phase Full Wave Rectifiers	38
3.9	Cascading of Diodes to Get a Higher PIV Rating.....	42
3.10	The Neon Transformer Output Connected to a Bridge Rectifier	43
3.11	Rectifier with Capacitor Filter.....	44
3.12	Power Supply with the Power Relays at the Output Before the Test Section.	46
3.13	An SCR in the On Mode (left) and Line Commuted SCR.....	48

3.14	The Voltage Divider and Digital Voltmeter Across the Capacitor	50
3.15	The Front and Rear Panel of the Control Box.....	54
3.16	Schematic of the Power Supply	55
3.17	Schematic of the High Voltage AC Power Supply's Top Panel.....	58
3.18	Circuit Showing the Current Limiting, Capacitor Discharging and Voltage Measurement Resistors.....	61
3.19	Current Measurement Circuit.....	62
4.1	Top and Side View of the Test Section.....	69
4.2	A Side View Showing the Imperfection in Level of the Lexan and the Steel Surfaces.....	72
5.1	Langmuir Probes, single (left) and double (right) types	76
5.2	Probe Characteristic Length	77
5.3	Single Probe Circuit	79
5.4	Dual Probe Circuit.....	79
5.5	The Probe Needles	80
6.1	Setup for Bench Testing.....	81
6.2	Voltage-Current Characteristics of Corona for the Test Section	83
6.3	Voltage-Current Characteristics for Negative Corona Before and After the Application of Ceramic Cement	84
6.4	Electrons Released from the Surface of the Insulator on the Cathode due to Malter effect.....	85
6.5	Side View of the Test Section Showing the Ceramic Cement Application Overlapped on the Wedge	86

6.6	The Waveform Picked up by the Ion Detector Probes.....	87
6.4	Proposed New Probe Circuit.....	88

LIST OF TABLES

Table	Page
3.1 Rectifier Performance Factors.....	40
6.1 Initial Bench Test Results	82

LIST OF ABBREVIATIONS and SYMBOLS

A, mA, μ A	Ampere, milli Ampere, micro Ampere
AC, ac	Alternating Current
Atm	Atmospheres
C	Coulombs
DC, dc	Direct Current
DPDT	Double Pole Double Throw (Relays and Switches)
DPST	Double Pole Single Throw (Relays and Switches)
ϵ_0	Permittivity of vacuum (and air) = 8.852×10^{-12} F/m.
e	Charge of an electron (1.602×10^{-19} C)
E_i	Ionizing Potential [eV]
eV	Electron Volt
E	Electric Field Intensity [V/m]
F, μ F	Farad, micro Farad
GTO	Gate Turn Off Transistor
H, mH	Henry, milli Henry
Hz, kHz, MHz	Hertz, kilohertz, megahertz
i_1, i_2	Currents of primary and secondary windings of transformer
i.d.	Inner Diameter
I_{dc}	DC current output of rectifier
in.	Inch
I_p	Probe current
I_s	RMS current output of transformer secondary winding
k	Boltzmann's constant (1.3807×10^{-23} J/K)

KE	Kinetic Energy
λ_D	Debye Length
LxBxH	Length x Breadth x Height
LED	Light Emitting Diode
m, cm, mm	metre, centimetre, millimetre
\overline{M}	Average mass of particles in a plasma
$n, n_e, n(v)$	number of, number of electrons, number of particles of velocity v
N	Total number of particles in a plasma
$N1, N2$	Number of turns of primary and secondary windings of transformer
NC	Normally Closed (relays and switches)
NO	Normally Open (relays and switches)
NC	Normally Closed (Relays and Switches)
NO	Normally Open (Relays and Switches)
$\Omega, k\Omega, M\Omega$	Ohm (Unit of Resistance), kilo Ohm, mega Ohm
o.d.	Outer Diameter
π	3.14159265
ϕ	Magnetic Flux [unit is Weber (Wb)]
Φ	Phase angle between voltage and current
ϕ_s	Plasma Potential
ϕ_p	Probe Potential
pf	Power Factor
PIV	Peak Inverse Voltage (rating for diodes)
P_{VA}	VA rating of the transformer
\mathfrak{R}	Reluctance [unit is Henry ⁻¹]
Re_1, Re_2	Power relays at the output stage of the HV DC power supply

R_L	Load Resistance
RMS	Root Mean Square
s, ms, ns	second, milli second, nano second
SCR	Silicon Controlled Rectifier
SPDT	Single Pole Double Throw (Relays and Switches)
SPST	Single Pole Single Throw (Relays and Switches)
T, T_e	Temperature, temperature of electron
U_p	Applied Probe Potential
UV, uv	Ultra violet
\bar{v}	Average velocity of particles in a plasma
V_1, V_2	Voltages of primary and secondary windings of transformer
V_3	Voltage across secondary of neon transformer
V, kV	Volt, kilo Volt
VA, kVA	Volt-Ampere, kilo Volt-Ampere
V_{dc}	DC voltage output of rectifier
V_s	RMS voltage output of transformer
V_r	Voltage read by digital Voltmeter across the Capacitor
W, kW, MW	Watt, kilowatt, Megawatt

CHAPTER I

INTRODUCTION

1.1 Plasma studies in Aerospace Engineering

In the simplest terms, plasma is ionized gas. Plasmas have received a lot of attention in aerospace engineering recently. Plasma studies took off in the 1920s and developed into a broad and specialized field. Integration of the aforementioned two disciplines will most likely result in numerous technological breakthroughs. A quick review of some recent research in this direction is presented below.

1.1.1 Previous Research

Studies in electro and magneto hydrodynamics have been progressing for applications such as propulsion, flow actuation and electric power generation. Miniature thrusters called Hall thrusters [1] as small as a few millimetres in diameter, have been developed, that use plasma for space propulsion. Hall thrusters accelerate plasma by applying an electric field in the direction of the flow and a magnetic field perpendicular to the flow. They can produce high thrust densities, with efficiencies of about 50%. Such propulsion devices can be used for manoeuvring small spacecraft or propelling small satellites.

An investigation on the electrohydrodynamic actuation of flow over a flat plate was performed by Artana et al., [2] for low speed air flows in the range of 11 to 17.5 m/s. The study used a high voltage dc (20 to 40 kV) to create a plasma sheet on the

surface of the plate. By altering the electric field intensity, the flow over the plate was shifted, causing changes to the size of the boundary layer. Thus it is possible to regulate the fluid to surface heat transfer and bring about drag reduction.

The effects of electrostatically generated plasma on shock waves were studied by Yano et al. [3], in wind tunnel tests at Ohio State University. Plasma was generated in the high pressure supersonic flow by high voltage dc corona discharge (>30 kV). Shocks were formed by the flow over a wedge. However, their results showed that there was no detectable shock mitigation due to the weakly ionized flow compared to a non-ionized flow. One interesting aspect of the study is that flow visualisation was made simpler due to the corona discharge, with the shock waves clearly visible in the glow and vivid colour pictures could be taken by a hand-held 35 mm camera. Some further work involving corona discharge is presented in chapter 2, after the phenomenon of corona discharge has been properly introduced.

1.2 Previous Plasma Related Work at UT Arlington

At the Aerodynamic Research Centre (ARC) of the University of Texas at Arlington several experimental studies have been conducted involving plasma in supersonic flows. Figure 1.1 shows the hypersonic shock tunnel [4] of the ARC in its original configuration. This shock tunnel was modified by replacing a part of the driven tubes with smaller diameter steel tubes. A specially made conductivity channel was constructed from copper plates so that the conductivity of the gas flowing through it could be measured. This setup, as shown in figure 1.2, is described in the paper by Stuessy et al. [5]

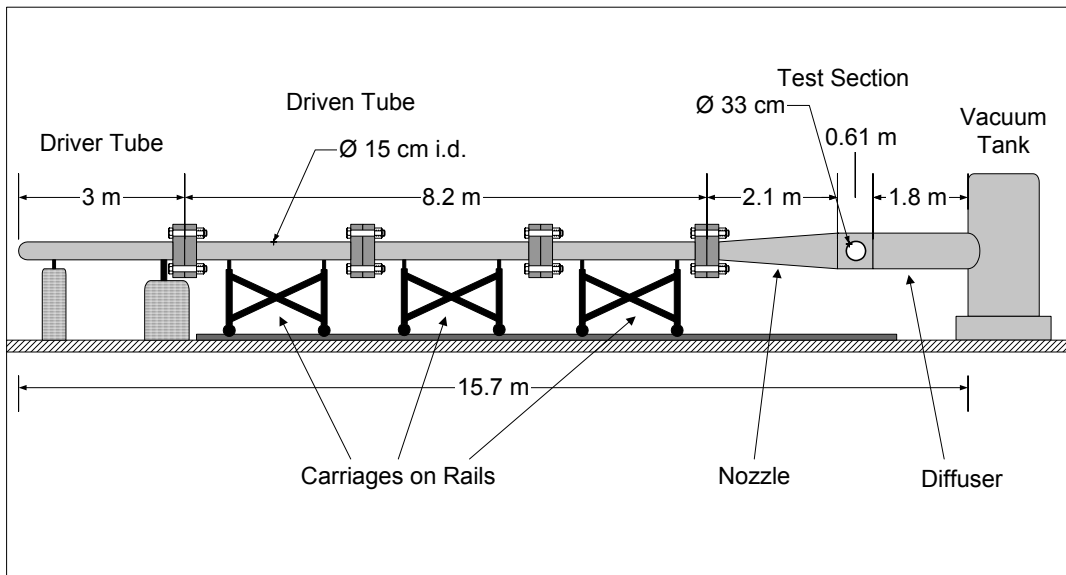


Figure 1.1: The hypersonic shock tunnel of the ARC.

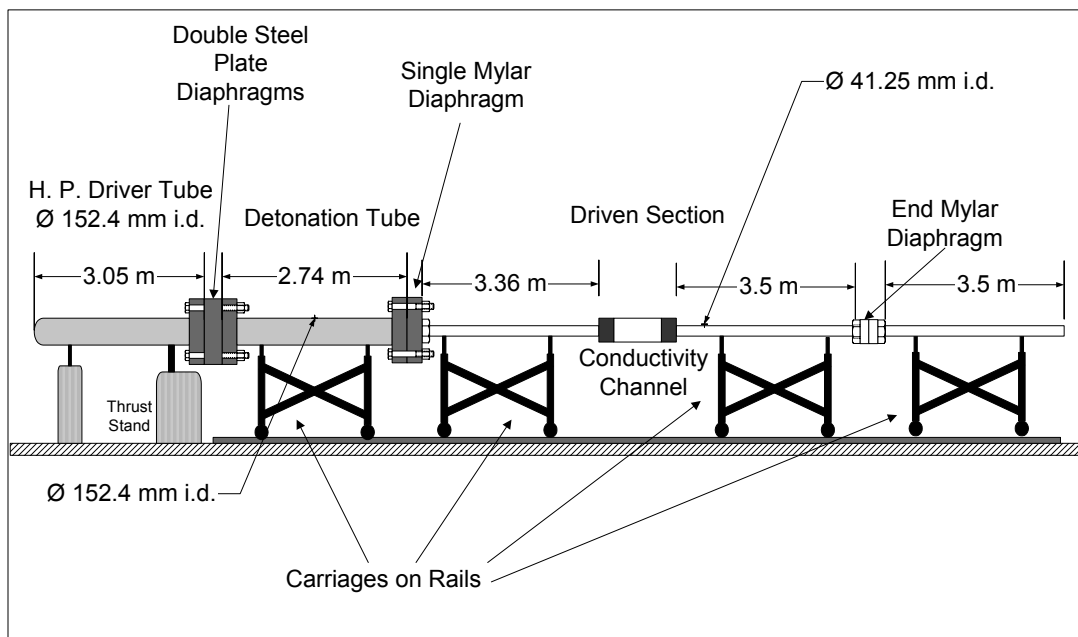


Figure 1.2: Schematic of the Detonation driven shock tube.

The conductivity channel experiments [6] consisted of detonating hydrogen and oxygen and seeding the combustion products with potassium carbonate powder. This combined mixture was blown down the driven tube by the force of the detonation. The fluid passed through the conductivity channel, across which a high voltage of 8kVdc

was applied, where the conductivity was measured and analysed. However, the results did not corroborate theoretical values of conductivity and measured values were found to be lower.

1.3 Brief Description of This Project

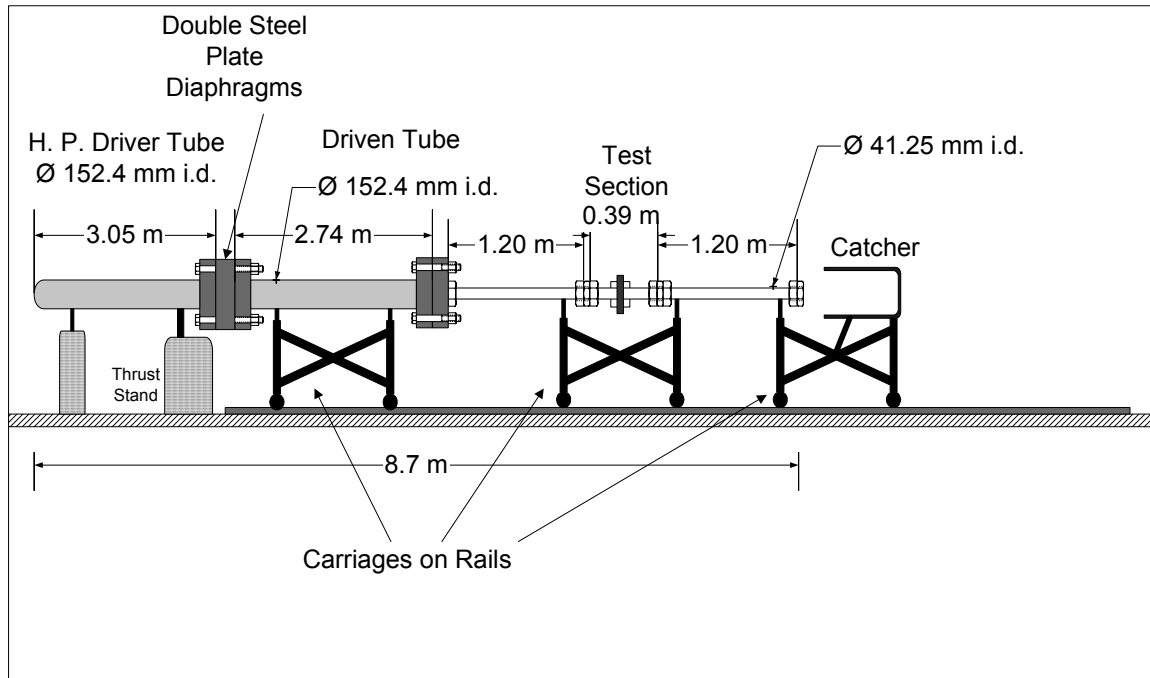


Figure 1.3: Schematic of the conventional shock tube.

This present study is part of a two-phase experimental investigation. Phase one involves:

- The building of the high voltage dc power supply and the test section, which is the device housing the corona discharge electrodes
- The determination of the voltage and current regimes for corona discharge for the test section
- Ionization of static and slow speed air
- The detection of ions in air using probes.

Phase two is the application of corona discharge in supersonic flows, to be carried out by Satyanand Udhyavar as part of his Ph.D. research. In phase two, the test section is to be fitted into the shock tube. When a supersonic flow is established through the test section, a high dc voltage is to be applied to the electrodes to induce corona discharge ionization. Probes introduced into the flow along the tube will detect ion current and voltages, to determine the ion density and temperature.

This project inherited a lot of the equipment and apparatus from the earlier tests carried out at the ARC. The supersonic tests are to be carried out in the same shock tube which has been modified to run in a conventional shock tube configuration, as shown in figure 1.3. The driver tube in this case can be filled with compressed air or helium. The test section is designed to fit into the driver section, such that it is electrically isolated from the rest of the facility.

As seen in figure 1.3, the shock tunnel now looks quite different from the earlier configuration. A large portion of the tubes has been removed. A catcher assembly was built to catch the high velocity flow as it blows out of the shock tunnel. The catcher is held in place by heavy chains, which are not shown in the picture.

Another major difference to the shock tunnel is the triggering mechanism for the data acquisition system (DAQ). Earlier, a trip-wire in the end Mylar diaphragm, shown in figure 1.2, was used to trigger the DAQ. The shortening of the shock tubes meant that this diaphragm could not be placed before the test section. A proposed technique is to use the signal from a pressure transducer to trigger the DAQ.

1.3.1 Applications for this Study

The ramifications of supersonic combustion engines are insufficient fuel-air mixing and inefficient combustion. The length of mixing and combustion chambers may be increased to counter this [7]. However, this solution adds its own problems of added weight, increased drag and reduced payload.

Ionizing the air-fuel mixture prior to combustion by means of high voltage corona discharge will result in the creation of free electrons, ions and free radicals in the air stream. This is a way to add enthalpy to the flow while making it more conductive and reactive. Thus lower energy is required to ignite the mixture in the combustion chamber. It is hoped that this will thereby increase the efficiency of the process. Corona discharge consumes very little electrical power. The electrical apparatus for the generation and sustenance of the corona can be designed to be very light weight and compact, saving weight and space, two important criteria for aerospace vehicles.

1.3.2 Overview of the Experimental Setup

Figure 1.4 shows a schematic of the corona discharge apparatus. The high voltage dc power supply has a variable output of 0-15 kVdc. The power supply is connected to the test section through a pair of high voltage control relays. The connectors of the power supply are such that the polarity of the output can be switched manually. A digital voltmeter on the output side reads the voltage being applied on the test section. A digital ammeter measures the current being delivered. These equipment are explained in chapter 3.

The test section consists of a steel tube with a triangular steel wedge inserted

through a cut-out section in the tube and held in place by supports made of Lexan [8], a plastic made by General Electric. Lexan also provides the electrical insulation between the two electrodes, that is, the wedge and the steel tube itself. The test section is described in chapter 4.

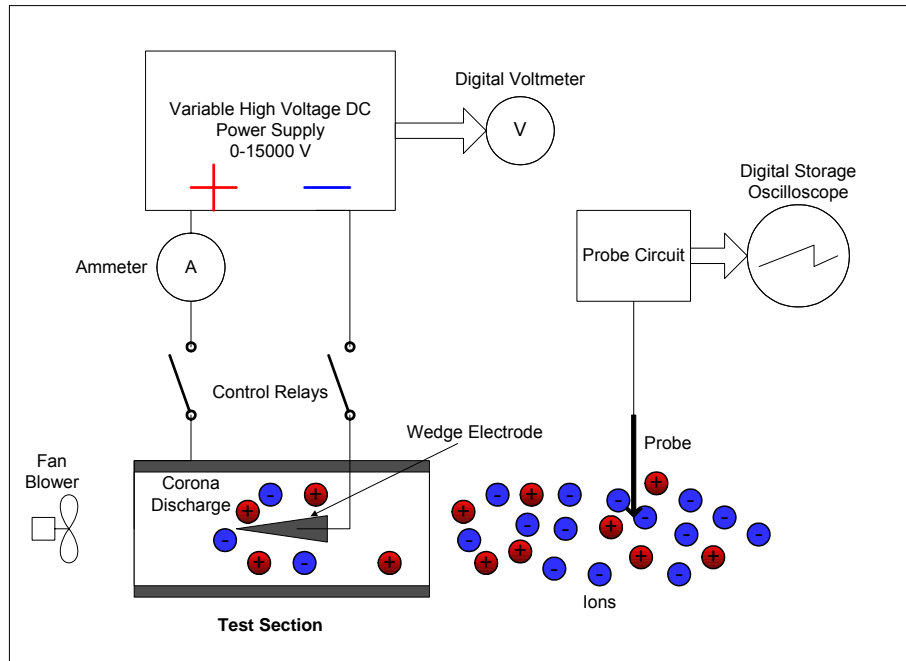


Figure 1.4: Schematic of the experimental setup.

When the contacts of the relays are closed, corona discharge takes place if the electrical potential is high enough. The ions produced diffuse outwards due to thermal and ionic convection or can be blown through the test section by a blower fan.

A probe placed outside of the tube detects the ions and the waveform is observed on a digital oscilloscope. The probe can be moved in an axial direction of the test section so that plasma properties can be measured spatially. The probe and the detection method are detailed in chapter 5.

CHAPTER II

THE CORONA DISCHARGE PHENOMENON

Before corona discharge can be explained, some basic concepts such as plasma and the phenomenon of ionization have to be introduced. This chapter is a brief and mostly qualitative description of these topics.

2.1 Plasma

There are five states of matter:

1. Solid
2. Liquid
3. Gas
4. Plasma
5. Bose Einsteinium Condensate

The first three are well known. The last one, BEC [9,10], is a state of matter predicted by Albert Einstein using mathematical formulations developed by Satyendra Nath Bose, in the early 1920s. It occurs when atoms, cooled down to a fraction of a degree above absolute zero, coalesce together to form a “super atom” that behave as one entity. BEC was created in a lab at the University of Colorado at Boulder by a team headed by Carl E. Wieman of UC-Boulder and Eric A. Cornell of the National Institute of Standards and Technology in 1995. They won the Nobel Prize in Physics in 2001 for this achievement.

Plasma is a gaseous mixture of free electrons and ions that have a high mean kinetic energy. The charge carriers influence each other due to their inherent charges and energies, and are also influenced by external fields. The physical properties of plasmas are notably different from that of other fluids that they have been classified as the fourth state of matter.

The term 'plasma' for ionized gas was introduced in 1927 by Irving Langmuir [11,12], the 1932 Nobel Laureate in Chemistry, because the way high velocity electrons, ions and particles flow in the medium reminded him of the way blood plasma carried corpuscles and other matter. Langmuir also invented the electrical probes that bear his name that are used to measure plasma properties such as charge carrier density and temperature. Langmuir probes will be examined further in chapter 5. Since the 1920s, plasma science has developed rapidly and has evolved into a field of its own. In industry today plasma is used in a variety of services some of which are to manufacture semiconductors and medical products, in lighting and lasers, welding technology and also in plasma based space propulsion systems. The potential application for the generation of plasma in this study is in supersonic combustion engines of the future.

About 99% of the universe is in the plasma state. Solar and stellar matter is plasma. These are classified as high temperature plasmas. Other examples of HTP would be the hot plasma created in nuclear fission and fusion reactions. On earth, plasma is found in the ionosphere, which can be grouped along with the aurora borealis or Northern Lights as low temperature plasma. Plasma also occurs in the atmosphere in lightning. The densities of plasma in the core of the sun and stars are very high, being

about 10^{30} particles cm^{-3} at a temperature of about 15 million Kelvin. In the solar corona plasma density is of the order of 10^8 cm^{-3} at temperatures of about 10^6 K. In fires and flames the plasma density is roughly at the same level but the plasma is at a much lower temperature. Arcs and lightning produce plasma of densities in the region of 10^{18} particles cm^{-3} with temperatures in the thousands of Kelvin. Fluorescent and neon lights produce light by exciting low pressure plasma in glass containers with densities of about 10^5 particles cm^{-3} and at temperatures of a few hundred degrees Celsius [13].

On the other hand, the plasma that is being generated in this study is of very low density, in the order of 10^6 cm^{-3} at low temperatures in the region of 300 K and may be termed weakly ionized gas.

2.1.1 Properties of Plasma

Neutral plasmas contain an equal number of positive and negative charge carriers, such that the net charge is zero. As a result of the charge carriers, plasma is a conductive fluid [14].

The most significant property of plasma is that it is strongly influenced by electric and magnetic fields. The effect of electric field on a charge is described by Coulomb's law

$$\vec{F}_E = q\vec{E} \quad (2.1)$$

where \vec{F}_E is the Coulomb force exerted on the particle of charge q in Coulombs and \vec{E} is the electric field in V/m. The force exerted on the charge is independent of its velocity.

The effect of magnetic field on a charge is expressed in Lorentz' law which is given as

$$\vec{F}_B = q\vec{v} \times \vec{B} \quad (2.2)$$

where \vec{F}_B is the Lorentz' force in N, exerted on a moving charged particle, q is the charge of the particle in C, \vec{v} is the velocity of the particle in m/s and \vec{B} is the magnetic field in T. The direction of this force can be determined by the right hand rule; the thumb shows the direction of the velocity, the index finger, the magnetic field and the middle finger, the force. According to Lorentz' law, with velocity there is a linear increase in the force exerted on the charged particle. Thus at high speeds, magneto hydrodynamics is a viable option for flow actuation.

Each charge carrier in the plasma simultaneously applies Coulombic forces on one another. This results in the strong force interactions and the formation of sheaths within the fluid. These properties of plasma explain why plasma is important to electro-magneto hydrodynamics [15].

2.2 Ionization of Air

A few methods of ionizing air or gas are mentioned below [16]:

1. Particle Impact Ionization
2. Thermal Ionization
3. Nuclear Emission
4. Photo or Irradiative Ionization
5. Electric Field Ionization:
 - (a) Arc Discharge Ionization
 - (b) Corona Discharge Ionization

2.2.1 Particle Impact Ionization

When an atom is struck by a particle, such as an electron or an ion, it can lose or gain a charge depending on the amount of energy transferred in the impact. This energy has to exceed the ionization energy E_i expressed in eV, where e (1.6×10^{-19} Coulombs) is the absolute value of the charge of an electron. In the case of electron impacts, the electron can be absorbed by the atom or it can cause the atom to lose electrons or just excite the valence electrons of the atom. An electron source is required to generate enough electrons to ionize the gas and sustain the electrons so that they last long enough to cause ionization and the electrons have to be accelerated by means of an electric or magnetic field. Electrons released in the ionization process can produce secondary ionization if their energies are high enough.

In place of electrons, ions can be accelerated and made to collide with and ionize atoms. Ions are heavier particles and therefore require much more effort to accelerate to attain the required ionization energy. This can be done in a particle accelerator or by means of strong electric or magnetic fields. Nuclear reactions emit ions that have high energies that can be used in ionization of gases. However this is not a safe approach for a study of ionization for supersonic flows.

2.2.2 Thermal Ionization

All matter above 10,000 K exists in the plasma state. And fire is filled with Ions and free radicals. If a gas is heated to suitably high temperatures the energies of the gas constituents become high enough to induce ionization within the medium. The requirement of such high temperatures and the problem of contaminants in air make this

an impractical approach for this study.

2.2.3 Nuclear Emission

Fusion reactions involving hydrogen emit H^+ and He^+ ions with very high energies in the order of MeV. Fission reactions of heavier atoms release high energy ions that can cause secondary ionization. However, this method of ionization would not be feasible for a small scale laboratory study. They cannot be adapted safely for application in a shock tunnel.

2.2.4 Photo or Irradiative Ionization

An ionisable atom can be ionized by the impact of a photon if the photon's energy $h\nu$ exceeds the ionization energy of the atom. Ultraviolet rays, x-rays and gamma rays are preferred for photo ionization. However, if the photon energy is far greater than the threshold ionization energy, the probability of ionization decreases. The degree of ionization is also lower for this method. Due to this fact and also the difficulty in adapting this technique to work in a shock tunnel, it is not viable for ionization of supersonic air.

2.2.5 Electric Field Ionization

This method involves passing the gas in between ionized electrodes. When the atoms or molecules come in contact with the surface of the metal electrodes, they lose or gain a charge subject to the polarity of the electrode. However, the electric field density has to be as high as a few kV/m to initiate ionization. The geometry of the electrodes is also important as electric fields around sharp objects and metallic surfaces with low radii of curvature are stronger than around blunt bodies. As the intensity of the

electric field is increased, the particles approaching the electrode are ionized before reaching it. The rate of ionization falls off as the intensity of the electric field is decreased. It is thought that at higher pressures and velocities of air, higher electric field strengths will be required. Electric field ionization is preferred because it is easy to generate and control high electric fields in the lab. Geometries of the electrodes can be varied and manufactured as desired.

When the intensity of the electric field increases beyond the breakdown potential of the gas, an arc discharge takes place. This is characterised by a heavy flow of current through the gas between the electrodes and high dissipation of energy in the form of heat followed immediately by a loud exploding sound. Although this method can yield high concentration of ions and higher charges of the ions (2+, 3+, 4+ or higher charges), it is not favoured because of damage to the electrode and apparatus, electrode heating, instability of the arcs and the high energy dissipation. Corona discharge is on the other hand, a low energy discharge that produces lower density ionization at the cost of a few mW of power. It is for this reason of low power consumption that this method of ionization has been adopted for this study.

2.3 CORONA DISCHARGE

Corona is derived from the French word for crown. Corona has been known for centuries by mankind, and often had supernatural properties ascribed to it. In Europe, it was known as St. Elmo's fire, named after St. Erasmus, the patron saint of sailors because it was often seen by sailors as a bluish-white flame on top of masts and sails of ships, often after a thunder storm, and was thus seen as a good sign from the gods. It

was reportedly seen by many sailors throughout history, including Julius Caesar, Magellan, Columbus and Charles Darwin, on his voyage aboard the H.M.S. Beagle. William Shakespeare even mentioned it in his play “The Tempest.” Corona is also seen on aircraft wing tips, propellers and antennae. Corona discharge is seen as a faint glow around high voltage conductors, especially on transmission lines around broken strands.

Corona discharge is used in air purifiers to clean air by ionizing the air. Ozone is a by-product of corona discharge and it is used to kill microbes and neutralize airborne contaminants. Corona discharge on transmission lines cause power loss and damage to the conductors and degrade the insulators. Thus power companies spend large sums of money to detect corona discharge on transmission lines and prevent them. Corona discharge on transmission lines has been known to cause radio frequency noise that interferes with communication signals. High frequency antennas are often fitted with a ball at the top to avoid ending in a sharp tip that is prone to corona discharge.

2.3.1 Features of Corona Discharge

Corona [17] is observed in many forms, including glows and haloes, spots, brushes and streamers. The potential at which corona is found to originate is called **corona threshold voltage**. Above this voltage, there is a limited region, in which current increases proportionately with voltage. This is called the **Ohm’s law regime**. After this region, the current increases more rapidly, leading to the complete breakdown and arcing or sparking at a point called the **breakdown potential**.

Corona discharge is highly dependant on geometry. Electric field intensity is higher around the surface of a charged conductor with higher curvature or lower radii of

curvature. If Q is the total charge stored in a conductor and r is its radius of curvature, the electric field intensity E is inversely proportional to the radius, as given by the following equation, where ϵ_0 is the permittivity of free space (and air) and is equal to 8.852×10^{-12} F/m.

$$E = \frac{Q}{4\pi\epsilon_0 r} \quad (2.3)$$

Therefore, as r decreases, the intensity of the electric field increases. This is why lightning conductors are made sharper and why antennas have to be protected from corona discharge.

When the electric field intensity increases, it affects the electrons in the atomic orbitals and may cause atoms or molecules to polarize or liberate electrons. The maximum electric field that a dielectric material can withstand without conduction is known as the **dielectric strength** of that material and is expressed in V/m or often V/mm. When the electric field increases beyond the dielectric strength, the material becomes conducting by a process called avalanche effect, whereby electrons collide with the atomic or molecular structure, releasing more electrons which in turn lead to the further breakdown of the material. Large currents are possible at breakdown. The dielectric strength of air at normal temperature and pressure is 3 kV/mm. At this point air ionizes rapidly and arcing occurs. This is what happens during a lightning strike. Corona discharge occurs below the breakdown potential, where the electrons are excited and release electro-luminescence. Therefore there is no massive destruction of the material.

An electron that is excited by an electric field E will ionize an atom or molecule of a gas if it has enough energy, called the **ionizing potential** of the particular gas, expressed in eV. This is shown as below.



Thus an extra electron is liberated in this process. However, if the electron does not have enough energy, it can impart a certain amount of kinetic energy to the particle it collides with:



This kinetic energy gained by the atom is released as photons having a certain energy and wavelength, resulting in the glow associated with corona discharges. If the energy of the photon is below that of the ionizing potential, it is absorbed by other atoms and may be re-released. If the energy of the photon exceeds the ionizing potential, the atom struck by the photon can release one or more electron depending on the energy level. This can result in a chain reaction, where by ionization is initiated in the gas.

Air is composed of nitrogen (78%), oxygen (21 %), argon (0.93 %), carbon dioxide (0.03 %), water vapour and particulate matter like dust, pollen, etc. One of the main products of corona is ozone. Oxygen ions are of the type O^+ , O_2^+ , O^- , O^{2-} and O_3^- . These combine to produce ozone. Molecular nitrogen also dissociates to form nitrogen oxides which are unstable that lead to reaction with oxygen to create more ozone. Water molecules produce ions of OH, H and O types of both negative and positive charges. Moisture content in the air increases its conductivity and tends to cause break down at a

lower potential. This is observed during thunderstorms leading to frequent lightning. Ionized air also contains free electrons. However, electrons being lighter have short life times and are absorbed by heavier particles and may result in the release of more electrons.

Dust particles are found to increase ionization rates. This has been observed in a phenomenon called **Malter effect** and experimentally verified in this study. This will be explained further in chapter 6.

When corona discharge is induced across two similar electrodes, it is called a bipolar corona. If one of the electrodes is made in a shape advantageous to corona discharge, i.e., with a lower radius of curvature compared to the other, a uni-polar corona is formed, as the corona discharge would be almost entirely concentrated around the electrode with higher curvature, which is termed the active electrode. If the active electrode is made positive with respect to the passive electrode, a positive corona discharge occurs. And if the active electrode is made the cathode, a negative corona is generated.

Corona can be generated by a high dc potential or ac, in which case it can be sinusoidal or pulsed, as shown in figure 2.1. Tesla coils, that generate dramatic corona discharge effects, operate at high frequencies of about 300 kHz. Corona has been found to be more intense at higher frequencies. Pulsed power is especially preferred for industrial applications. In the case of pulsed power discharges, the duty cycle of the waveform can be modified to alter the power consumption or the rate of ionization. Also the dc offset can be changed to vary the effects.

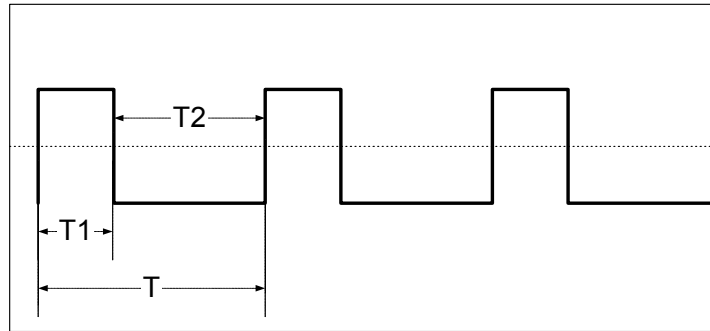


Figure 2.1: A Pulsed power waveform.

2.3.2 Corona vs. Arcs and Sparks

Corona occurs at high electric field intensities, but lower than the dielectric strength of the medium. Therefore, it is a low current, low power discharge with a low intensity photo emission. Arcs and sparks occur when the dielectric strengths have been crossed. Thus they essentially short out the voltage, creating a high current, high power discharge, with high heat and luminescence.

Corona discharge is sustained over a longer period of time, as long as the electric field is applied. Arcs and sparks are quickly extinguished, as the energy stored in the source of the electric field is dissipated by the discharge.

The heating caused by corona is not as significant as that of arcs and sparks, although it is a cause of concern to power companies, where miles and miles of transmission lines can create a significant loss by corona discharge over a long period of time. Corona discharge dissipates a few W of power, but usually much below that, in the region of mW or less. However, arcs can consume hundreds, thousands or more W of power in the fraction of a second.

Corona is faintly visible in the shorter visible wavelengths, in the blue and violet range, but most of it is UV. Heating can be observed by infra red cameras. Arcs and

sparks are mostly visible and they release waves in the UV through infrared spectrum.

2.3.3 Earlier work involving Corona Discharge

Many studies have been done involving corona discharge both in aerospace fields as well as others that might be noteworthy to the present study. These are briefly described below.

Anikin et al. [18], performed experimental and numerical studies to create plasma by applying pulsed high voltage in atmospheric (1 atm) and low (0.1 to 30 Torr) pressure air. The set up was a cone shaped positive electrode, whose distance from the passive electrode, a flat disk could be varied from 0 to 30 cm. The corona was detected by optical means. At 1 atm pressure, the pulse was in the form of a fast rising peak of 75 ns duration and frequency of 1.2 kHz. The peak amplitude was 9 kV. Anikin et al. observed streamers that increased in intensity with the voltage. For low pressure air, voltage pulses of 10 to 15 kV were applied, with a duration of 25 ns, for which high velocity ion and electron generation were observed. Another significant observation made was that as the pressure increases the electric fields have to be increased in order to generate a corona. The same research team has applied this high frequency fast ionization wave technique in ignition of hydrogen and hydrocarbon fuel-air mixtures [19].

Shale et al., [20] studied the characteristics of positive corona at various pressures (0 to 80 psig) and temperatures (600 to 1500 °F). They studied the voltage vs. pressure and temperatures behaviour from the onset of corona to arcing. It was found that positive corona demonstrated a higher arc-over voltage, thereby giving a wider

range of operability for positive corona over negative corona. Also, for positive corona at higher densities, the current flow decreased for a constant voltage.

Several interesting work applying corona to automobile engine combustion and diesel exhaust treatment have been done at the University of Southern California. Gundersen [21] has studied the use of corona discharge for the initiation of combustion in combustion engines. He concluded that corona has certain distinct advantages over arc combustion, including better coupling into the gas of the energy, lower radiation losses, and lower losses due to gas dynamic disturbances. Work on treatment of diesel exhaust has also delivered positive results.

Vinogradov et al. [22], have studied the effect of uni-polar corona discharge on a flame. They found that the height of the flame decreased with increasing field intensities, with total quenching of the flame at certain high field strengths. Chernikov et al. [23], have performed experimental investigations to study the effect of corona discharges in supersonic air-propane mixtures. They found that there was no significant improvement in the formation of radicals of OH, CH, O and H₂ in the flow due to the discharge; however, there was an increase in the electron density in the flow. They concluded that such discharges can be used for ignition of fuel in ramjets.

Ekchian et al. [24], have tested a device that can be retrofitted onto gasoline or diesel engines to produce corona discharge in the exhaust. They found that this produces radicals in the exhaust that increase the efficiency of the catalytic converter to weed out pollutants.

CHAPTER III

DESIGN OF THE HIGH VOLTAGE POWER SUPPLY

3.1 Requirements of the Power Supply

The power supply that was required for this project had to do the meet the following criteria:

1. It should supply a variable output dc voltage from 0 to a ceiling of not below 15 kV, current flow of about 10 mA, with no appreciable drop in voltage
2. The polarity of the output voltage should be easily interchangeable
3. The output voltage should be continuously variable
4. The output supply must be able to be turned on and off from a remote location
5. The output current should be limited so that the test section is not damaged severely
6. The output voltage and current should be measurable to a high degree of precision
7. The system should be easy to use, robust and easy to maintain
8. The high voltage equipment should not produce electrical or radio frequency disturbance that can affect apparatus in the vicinity
9. It has to be built within the budget allotted to the project, which was rather limited
10. It should be safe to people and equipment in the surrounding area.

3.2 Types of High Voltage Generators

There are plenty of ac to dc converters and switch mode power supplies available and are easy to make; however, these are all low voltage supplies, typically below 200 Vdc. The difficulties of manufacturing a high voltage dc power supplies are numerous, including, procurement of devices rated at high voltages, insulation and isolation of components from each other, just to name a few. High voltage dc power supplies of various ratings and sizes are available from commercial manufacturers, but they cost thousands of dollars, which was one resource that was limited. Many common machines and appliances contain high voltage generating devices within them, such as television sets and computer monitors, microwave ovens and automobile ignition systems, that may be modified to use as high voltage power supplies. However, they do have their limitations.

Some of the various high voltage power supplies that were considered are briefly described below:

- Voltage Multiplier Circuit
- Van de Graaff generator
- Tesla coils
- Step up transformers and rectifiers circuits
 1. Microwave oven power supply
 2. Television and computer monitor Flyback transformers
 3. Ignition transformers

3.2.1 Voltage Multipliers

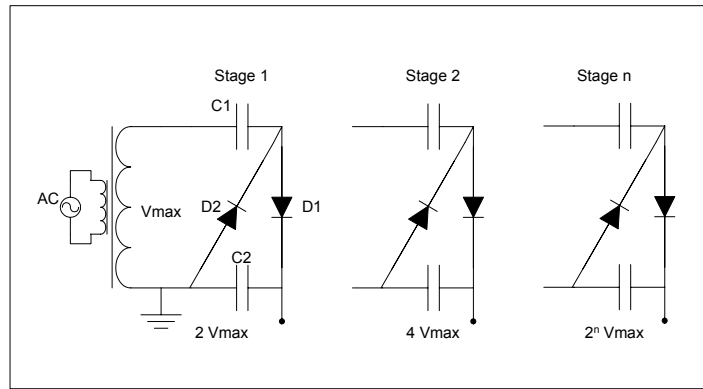


Figure 3.1: Voltage Multiplier circuit.

Voltage Multipliers [25] are circuits that convert ac to dc and then multiply the output several fold. These are widely used to power digital circuits; however voltage multipliers built with high voltage/current rated components can be made to deliver as high a voltage as required. The basic voltage multiplier circuit is shown in figure 3.1. Each stage consists of two capacitors and two diodes connected to an ac source, as shown. During the positive half cycle, the top side of the transformer secondary winding in the picture is positive and current flows through capacitor C1 and through diode D1 and capacitor C2 back to the secondary winding. Thus capacitor C2 charges to V_{\max} . During the negative half cycle, the bottom side of the transformer winding is positive and the top is negative. Therefore, diode D1 being reverse biased does not conduct. However, diode D2 is forward biased and conducts through C1. Thus C1 is charged to V_{\max} . During the next positive half cycle, V_{\max} from the transformer as well as the voltage V_{\max} present in C1 is now applied across C2. Thus C2 charges to $2V_{\max}$. The output is obtained across capacitor C2. Several stages of the multiplier circuit can be cascaded to obtain $2^n \times V_{\max}$.

There are several drawbacks of this circuit. As load current from the output capacitor is drained, the voltage across it drops. Therefore, these voltage multipliers can be used for very low current applications only. It is not possible to get a continuously variable output voltage. Output voltage can be varied in steps only. For lower frequency supply voltages, there is an increasing voltage drop as the number of stages is increased. The cost of assembling a high voltage version of this circuit is high as many capacitors and diodes are required.

3.2.2 Van de Graaff Generator

The Van de Graaff generator (VDG) [26] was invented by Robert Jemison Van de Graaff, the American physicist, in the 1920s. This electrostatic charging generator works by building a static charge on a sphere from a rolling belt made of a non-conducting material such as rubber or nylon. VDGs are capable of generating as high as 20 MV with very low currents in the range of μA or lower. The voltage is a function of time, that is, the longer it runs, the higher the voltage. However, a VDG is a constant current source and supplies a constant feeble current until the entire charge build up is drained. But as the current is drained, the voltage drops. Therefore, it is not a viable dc power source as it is difficult to control the output voltage accurately and the currents are too weak.

3.2.3 Tesla Coil

Tesla coils [26] are high voltage generators that generate high voltages of high frequencies (100s of kHz). The secondary of the Tesla coil is not wound on a metal but air cored. The primary side of a resonance transformer is in series with a capacitor

forming an LC circuit. The primary side is supplied with a high ac voltage (a few kV) usually of line frequency (60Hz) from a step-up transformer. One end of the secondary coil is grounded while the other is connected to a sphere or a toroid that is kept off the ground. This creates a capacitance with the ground, thus forming another LC circuit. When both the primary and the secondary LC circuits are tuned to the right frequency, which is done by changing the turns ratio on the primary, a standing wave of the right frequency is amplified to a high voltage on the secondary. Tesla coils that are 5 feet high can reach as high as 300 kV, while miniature ones can generate up to 50 kV. They are used to generate sparks of a few inches to a few feet in length depending on the voltage output. However, it is hard to control the output voltage and the output voltage cannot be rectified to obtain a steady dc voltage.

3.2.4 Step-Up Transformer and Rectifier Power Supply

The simplest power supply is to step up an ac voltage with a transformer and to rectify the output using diodes and filter with a capacitor [27]. The ac voltage is available from the domestic 120 V, 60 Hz supply. Some of the high voltage transformers that are commonly available are described below.

3.2.4.1 Fly Back Transformers or Line Output Transformers

Television sets and computer monitors that have a cathode ray picture tube in them operate on very high voltages, about 24 kV or sometimes even higher than 30 kV, depending on the size of the screen. Such high voltages are used for accelerating the electron beam, horizontal deflection of the beam about the screen for scanning and focusing the beam. This voltage is generated by a special transformer known as the

Flyback Transformer (FBT) or Line Output Transformer (LOT) [28]. The name Flyback originated from the fact that the output of this transformer is used to move the electron beam back to the start of a new line on the screen once the scanning of a line has been completed.

The FBT has several windings on both the primary and secondary side. The secondary side is tapped at numerous points to get different levels of voltages, with the highest for beam acceleration and horizontal deflection. FBTs are made of coils of very fine wire, wound on a ferrite core with an air gap. Thus it is able to store energy in the air gap and works as an inductance. The output of the transformer is rectified with diodes and filtered with capacitors. Some CRTs have FBTs that deliver around 8 kV which is then multiplied with a voltage multiplier circuit, similar to the ones discussed before, to obtain the higher voltages.

The features that distinguish FBTs from other transformers are given below:

- FBTs have an air gap that store energy in them, making them pure inductors, and also giving them a higher reluctance than regular transformers.
- The current flow in the primary and secondary coils is out of phase with each other.
- The voltages applied to the FBTs are usually rectangular in shape, while the current flow is usually triangular in shape.
- FBTs operate at high frequencies in the range of from a few kHz to the lower MHz. Therefore, the diodes and capacitors used in the rectification process are not very bulky. However, operating them at lower frequencies will cause their

cores to saturate, limiting the current drawn from them and can make them susceptible to failure. The core saturation can be a safety mechanism in cases where the secondary is shorted, in case of an arc for example, whereby the current is limited and the transformer winding may not burn away or blow a fuse.

- The normal operating current output of FBTs are very low, in the low milliamps range.
- The high frequencies required make it necessary to build a more complicated control circuit.
- These reasons render FBTs unsuitable for a power supply application for this project.

3.2.4.2 Microwave Oven Power Supply

Microwave ovens have a transformer and diode rectifier system. The Microwave Oven Transformer (MOT) is capable of generating about 2 to 3 kV at 1 to 4 kW depending on the oven's model and power rating. These transformers are used to drive the magnetron that produces the microwaves, with enough power to heat food. The MOTs are not current limited by core saturation and are therefore dangerous in case of shorting of the secondary. However, the voltage requirement of this project is up to 15 kV and therefore, cascading of several transformers in series would be necessary. This is also dangerous because the insulation on the MOTs may not hold up to higher voltages than they are rated at.

3.2.4.3 Ignition Transformers

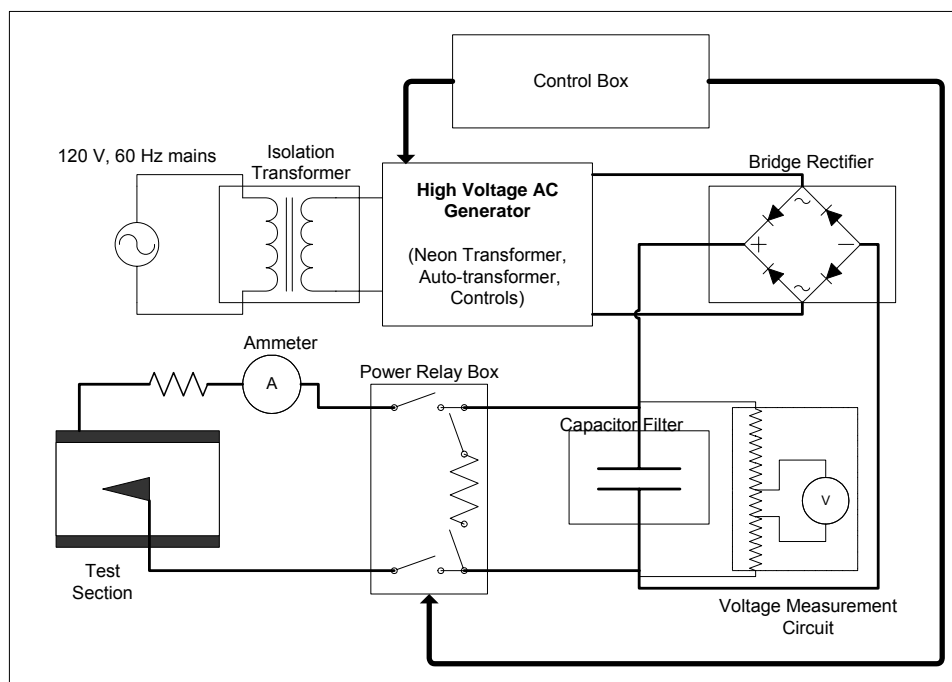
Fuel Oil Ignition Transformers are used in fuel oil burning heaters to ignite the fuel with an arc. They are usually rated at 10 kV, 20 mA. They are constructed with the secondary winding centre tapped to the core, which is then grounded. These transformers are also current limited by the core, if their secondary windings are shorted but will eventually burn up due to the heat generated. They can be cascaded in parallel or series to get higher currents or voltages. These are also a good choice for building a high voltage power supply.

Automobile ignition coils can produce about 30 kV ac. They have a primary and a secondary coil wound on an iron core. They also have internal connections between the primary and secondary coils that are switched to create the high voltage output across the secondary. They are designed to work on 12 or 24 volts and therefore require a high frequency switching control circuit. This can create high frequency transient noise in the system. They require a complicated circuit to obtain a variable voltage output. Although these can be cheaply bought at a vehicle scrap yard, they are not a good choice for a high voltage dc power supply.

3.2.4.4 Neon Transformer

After studying all these options, the conclusion drawn was that the best choice is to use a neon light transformer to step up the input voltage and then rectify the output with a bridge rectifier and filter it with a simple capacitor filter. This setup is shown in figure 3.2. The ac mains supply is connected to the high voltage ac generator through an isolation transformer, with 1:1 turns ratio. This is to isolate the high voltage side from

the line. The high voltage ac generator consists mainly of a variable autotransformer that supplies the input to the neon transformer. The output of the neon transformer is connected to a bridge rectifier containing four high voltage diode assemblies. The rectified output is filtered and stored in a large 1 μF capacitor. The voltage across the capacitor is measured with a high resistance voltage divider (500 $\text{M}\Omega$) with 100:1 input to output ratio, by a high input impedance digital voltmeter. The power is applied to the test section through a pair of Normally Open (NO) power relays. Another pair of relays, Normally Closed (NC) type, is used to discharge the capacitor. A power resistor of 1.1 $\text{M}\Omega$ is used to limit the current supply. Current flow in the circuit is read by a digital voltmeter reading the voltage across a 10 Ω resistor. All these components are further



explained in this chapter.

Figure 3.2: Schematic of the High Voltage DC Power Supply.

3.3 The Neon Transformer

Neon lights and luminescent tubes, used in commercial displays and on bill boards, are glass tubes filled with low pressure inert gases like neon, argon, krypton, etc. They produce luminescence when the gases are excited by a high voltage applied across the tubes. The different colours are characteristic of the gas inside the tubes. Neon gives off a red colour, while a mixture of argon and mercury gives off a light blue colour [29].

The high voltage is applied by means of a special step up transformer, known commercially as a neon transformer. Neon transformers are available in a variety of sizes. They are rated for their secondary open circuit voltage and short circuit current, i.e., the listed voltage is the maximum voltage when no load is applied across the output terminals and the listed current is the highest current that can be drawn from it. However, this happens when the secondary is shorted, that means the effective output voltage is zero.

The secondary open circuit voltages, short circuit currents and power ratings of some of the common types are listed below.

9000 V	270 VA	30 mA
	540 VA	60 mA
12000 V	360 VA	30 mA
	720 VA	60 mA
15000 V	450 VA	30 mA
	720 VA	60 mA

The primaries are available in 120 Vac, 60 Hz for the US or 240 Vac, 50 Hz for Europe. A transformer with primary/secondary rated as 120 V/12000 V would have a turns ratio of 100. Thus any voltage input to the primary would be stepped up 100 times on the secondary. The model used for the power supply is a 120/12000 V, 720 VA, 60 mA, 60Hz transformer manufactured by Franceformer [30].

The design of the power supply is such that the maximum output voltage and currents can be changed by replacing the transformer with one with the required power rating. A 120/12000V, 360VA transformer and a 120/15000 V, 450 VA transformer, both from Franceformer, are also available here at the ARC that can be used in the power supply if required.

3.3.1 Normal Power Transformer Operation

The operation of a normal power transformer is described below [31]. If the number of turns on the primary and secondary windings are denoted by N_1 and N_2 respectively and the voltage applied to the primary is $V_1(t)$ and the current flowing through the two windings are $i_1(t)$ and $i_2(t)$ respectively, the Reluctance \mathfrak{R} of the magnetic circuit and the flux ϕ in the core is given by the following equation.

$$N_1 i_1 - N_2 i_2 = \mathfrak{R} \phi \quad (3.1)$$

Reluctance \mathfrak{R} for a core of length l and cross sectional area A and permeability μ of the material is given by

$$\mathfrak{R} = l/\mu A \quad (3.2)$$

For iron, μ is $5000 \mu_0$ ($5000 \times 4\pi \times 10^{-7} \text{ H/m} = 0.0063 \text{ H/m}$). For an ideal transformer, the right hand side of equation 3.1 is zero as $\mu \rightarrow \infty$.

$$i_1/i_2 = N_2/N_1 \quad (3.3)$$

$$v_2/v_1 = N_2/N_1 \quad (3.4)$$

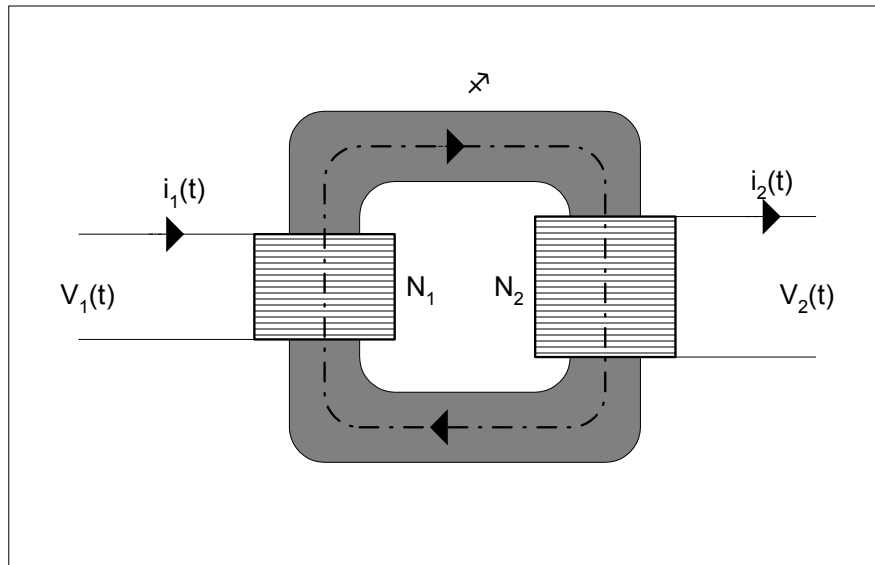


Figure 3.3: Schematic of a transformer.

3.3.2 Power Factor

For a dc supply, power

$$P = VI \text{ [Watts]} \quad (3.5)$$

For an ac circuit, the current may be out of phase with voltage. Therefore, power is expressed in VA (Volt Amperes) as shown below, where Φ is the phase difference between voltage and current.

$$P = VI \cos\Phi \text{ [VA]} \quad (3.6)$$

The term $\cos\Phi$ is known as power factor. This is important for ac circuits, especially transformers, because inductive circuits tend to create a current phase lag and lower the phase difference, while capacitive circuits tend to create a voltage phase lead and increase the power factor, but never more than unity. Lower power factor means that

more current is required to maintain the power requirement. DC circuits have a power factor of 100 %.

Transformers and other appliances rated Normal Power Factors have 40 to 50 % pf. Those rated as High Power Factor has at least 90% pf.

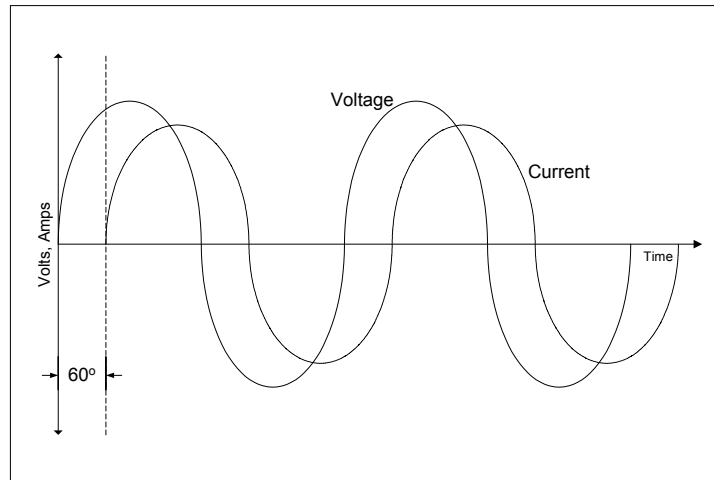


Figure 3.4: Current lagging voltage by 60°.

3.3.3 Features

Neon transformers have a different construction and operation scheme from that of normal power transformers. Neon transformers have an iron core. The secondary windings are done in two parts, and they are connected in series internally. In effect there are two secondary windings. One end of each secondary winding is shunted to the iron core. The iron core thus forms an electrical path for joining the two secondary windings and is the centre tapping on the secondary winding. A terminal connected to the iron core is available on the outer box. In neon light applications this is usually grounded.

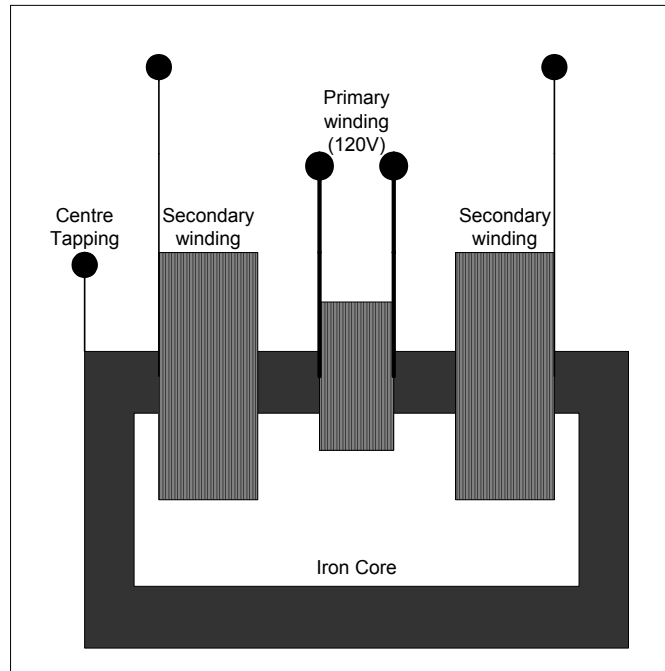


Figure 3.5: Schematic of a neon transformer.

Neon transformers have low output voltage regulation, i.e., the output voltage will fall with increase in current drawn. This is the biggest drawback of using the neon transformer for a high voltage dc power supply. However, this can be somewhat solved by adding a fairly large storage capacitor to the output of the rectifier.

The neon transformer has a normal pf rating, i.e., 40 to 50 %, due to the magnetic shunting and the secondary windings. Neon transformers with power factor correction are available. Power factor correction can be done by connecting a capacitor across the primary, thus reducing the current drawn by the primary in almost half.

Neon transformers have a built in safety feature of current limiting. When the secondary windings are shorted, only a limited current will flow through it, because the iron core, which is magnetically coupled with the windings, gets saturated and presents a high reluctance to the magnetic flux induced by the current, which in turn limit the

current flow. This feature protects the winding of the transformer from burning out during an arc discharge, and also offers some degree of protection to the power devices like diodes and capacitors in the power supply circuit.

The neon transformer core and winding assembly is covered with an insulating compound, such as asphalt or epoxy resins and housed in a steel box with the terminals isolated on ceramic stand offs. The metal container is connected to the core and is therefore the centre tapped ground.

3.4 The Autotransformer

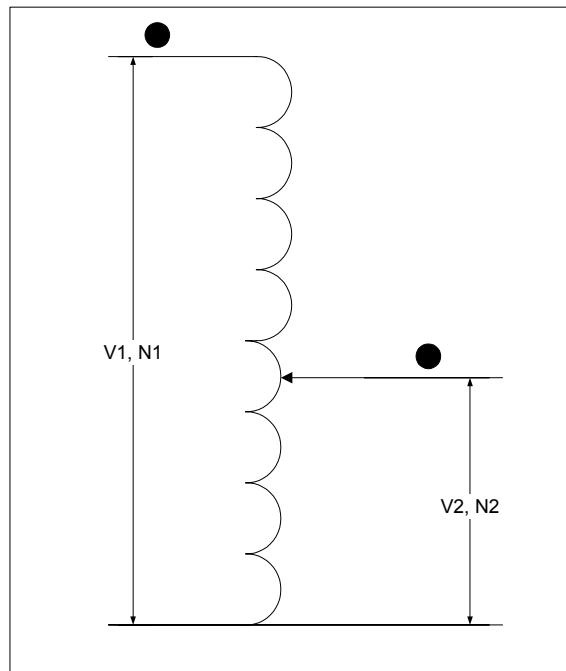


Figure 3.6: The circuit diagram of an autotransformer.

The variable autotransformer, also known as a variac, is a simple single coiled inductor. The output is varied by moving a sliding contact across an exposed section of the coil. The two dots show the phase of the input and output. The output voltage is obtained as a turns ratio.

$$V_2 = V_1 N_2/N_1 \quad (3.7)$$

The power rating of the autotransformer used in the power supply is 1.7 kVA. The output of the autotransformer is connected to the input of the neon transformer. The output of the neon transformer is thus

$$V_3 = N V_2 \quad (3.8)$$

where N is the turns ratio of the neon transformer. In the case of the 12 kV secondary, 360 VA neon transformer, the output is given by

$$V_3 = 100 V_2 \quad (3.9)$$

Note that these voltages shown above are ac RMS values. Thus dc values will be much higher. Thus a theoretical 100 times magnification of the input voltage is obtained. However, with the neon transformer this is not exactly true. There is a slight drop in the output voltage. This is not a worrying issue as the highest voltage attainable is much higher than the maximum required voltage. With the 12 kV neon transformer connected in the power supply, the dc output was found to be about 16 kV.

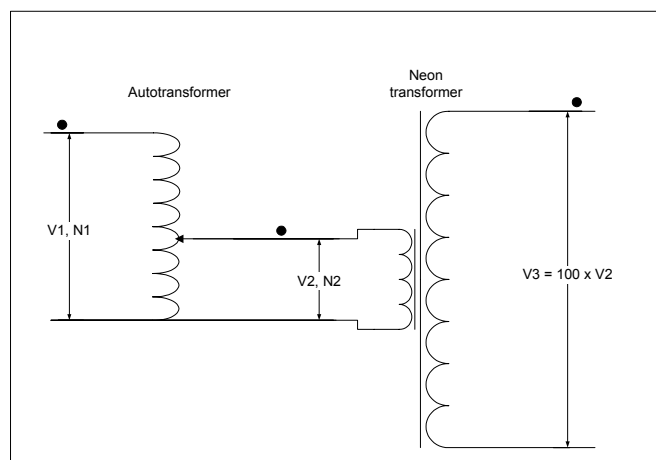


Figure 3.7: Connection of the autotransformer to the neon transformer.

3.5 The Diodes

The simplest way to convert ac to dc is by rectification. For high power dc supplies like welding sets, three phase rectification is carried out. This would reduce ripples significantly. Since the neon transformer is a single phase one, the full wave rectification is preferable.

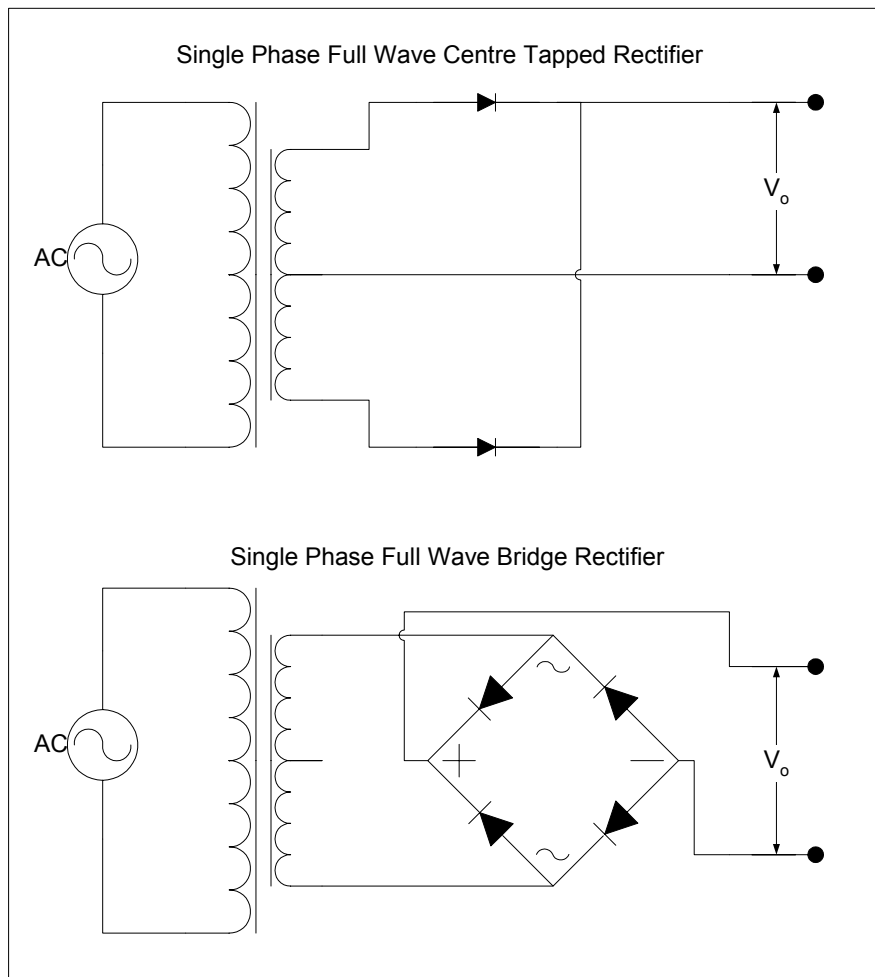


Figure 3.8: Single phase full wave rectifiers.

Some of the factors used to compare rectifier circuits are briefly explained below [25].

Efficiency: Conversion efficiency of a rectifier is the ratio of dc power delivered to the

load to the power supplied to it by the transformer. Efficiency should be as close as possible to 100 %.

$$\eta = \frac{P_{dc}}{P_{ac}} = \frac{V_{dc} I_{dc}}{V_{rms} I_{rms}} \quad (3.10)$$

Ripple Factor is a measure of the effectiveness of the rectifier to convert ac to dc. It is the ratio of the effective ac voltage or current to the average value of the voltage or current. Ripple factor should be ideally as close as possible to zero.

$$RF = \sqrt{\left(\frac{V_{rms}}{V_{dc}}\right)^2 - 1} \quad (3.11)$$

Form Factor is a measure of the shape of the output voltage and is a ratio of the effective value of the output ac voltage to the output dc voltage.

$$FF = \frac{V_{ac}}{V_{dc}} \quad (3.12)$$

It should be as close to zero as possible.

Peak Inverse Voltage (PIV) is the maximum reverse voltage that is applied across the rectifier during the negative cycle.

Transformer Utilization Factor (TUF): The utility factor of a transformer supplying current to a rectifier is the ratio of the dc power output of the rectifier to the rated RMS Power capacity of the transformer secondary. This is not to be mistaken for efficiency, because here the ratio is based on the rated VA of the transformer, not what is actually delivered to the rectifier.

$$TUF = \frac{P_{dc}}{P_{VA}} = \frac{V_{dc} I_{dc}}{V_s I_s} \quad (3.13)$$

V_s and I_s are the RMS voltage and current rating of the transformer. V_{dc} and I_{dc} are the dc voltage and dc current output of the rectifier.

Transformer VA is the equivalent capacity of the transformer secondary compared to what it would be if it were delivering a pure ac voltage. It is the inverse of *TUF*.

Harmonic Factor is a measure of the distortion of a waveform. An ideal rectifier has no voltage drop across the diodes, 100 % efficiency, $V_{ac} = 0$, $RF = 0$, $TUF = 100 \%$, $HF = 0$, power factor = 1.

Table 3.1: Rectifier performance factors.

Rectifier	Efficiency	Ripple Factor	Form Factor	PIV	TUF	Transformer VA	Fundamental Ripple Frequency
Half Wave	40.60%	121%	157%	$1.414 V_{max}$	0.286	3.496	60 Hz
FW CT	57.50%	48%	111%	$1.414 V_{max}$	0.67	1.75	120 Hz
FW Bridge	81.20%	48%	111%	$0.707 V_{max}$	0.813	1.23	120 Hz

From the above table, it is clear that the bridge rectifier is a better choice. A few more advantages and disadvantages of the bridge rectifier are listed below.

Advantages:

- No centre tapping is required. Therefore, a higher voltage is available from the transformer for rectification.
- This is more robust, since the diodes only take half the peak voltage across the transformer during any half cycle.
- There is a higher transformer utilization factor, as the whole transformer is used rather than one half of the secondary winding.

Disadvantages:

- More number of diodes are required for the bridge configuration, four vs. two in

the case of the centre tapped FWR.

- Diodes have a voltage drop across them and in bridge rectifier setup, the drop across two diodes in each phase has to be accounted for.
- Since there are two diodes during each phase, the diodes can be rated at just above the peak voltage. In CTFWR, since only one diode is conducting and if there is a capacitor in parallel across the output, the diodes have to be rated at two times the peak voltage, thus requiring higher rated diodes.
- If one of the diodes fails, the bridge rectifier reverts to being a half wave rectifier. However, it is the same case with the centre tapped FWR also.

For high voltage rectification, vacuum tubes work remarkably well. Most of them are rated for high voltages and handle fairly large currents. However, they have a few drawbacks. They require a filament heating supply and it takes a few seconds for the filament to get hot enough for proper functioning of the tube. Their switching times are slower than solid state devices. Tube rectifier circuits are usually connected in a full wave centre tapped configuration, as tubes do not work well in series and the voltage drops across them can be rather large. Although, it would seem out of the ordinary to adopt an older technology, the incentive for using vacuum tubes is that they can be bought cheaply from individual sellers and old equipment retailers.

On the other hand, solid state diodes are more reliable and easy to handle, not having to care about breakage of glass or loss of vacuum. Solid state diodes are available in all ratings. However, the faster and higher voltage or current rated diodes are more expensive.

Diodes have a current rating and a Peak Inverse Voltage (PIV) rating. High voltage diodes are also found in several common appliances. Microwave ovens, television sets, and computer monitors etc. use diodes for rectification. These can be purchased at spare part shops. However, their current ratings might be too small or the voltage ratings may not be high enough. It is safer to have diodes at least twice the highest voltage required.

One way to use lower rated diodes is to cascade several diodes till a favourable safety factor is achieved. For example if the diode has a PIV rating of V_d , several may be cascaded as shown in figure 3.8, to get a PIV of $n \times V_d$.

However, at high voltages, corona losses and arcing can occur between the terminals. Therefore, it is necessary to ‘pot’ the diodes by covering them with an insulating material like silicon sealant or epoxy or immerse them in non-conducting oil. Another downside to cascading diodes is that the voltage drop across each diode in the series adds up. It can be a significant drop in case of high voltage diodes.

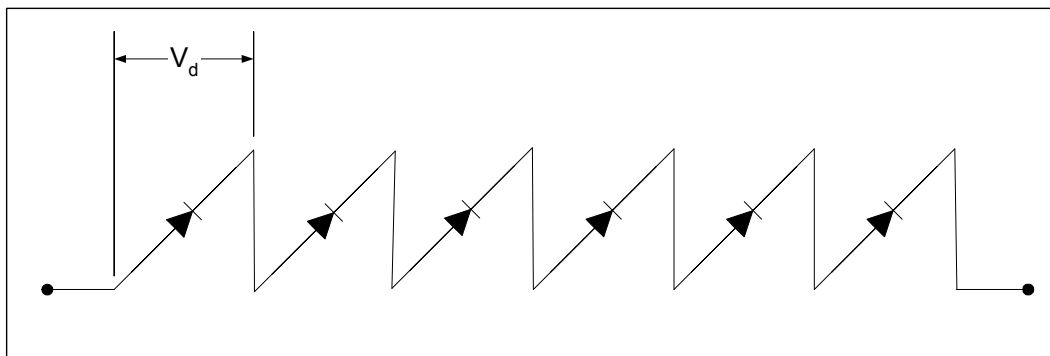


Figure 3.9: Cascading diodes to get a higher PIV rating.

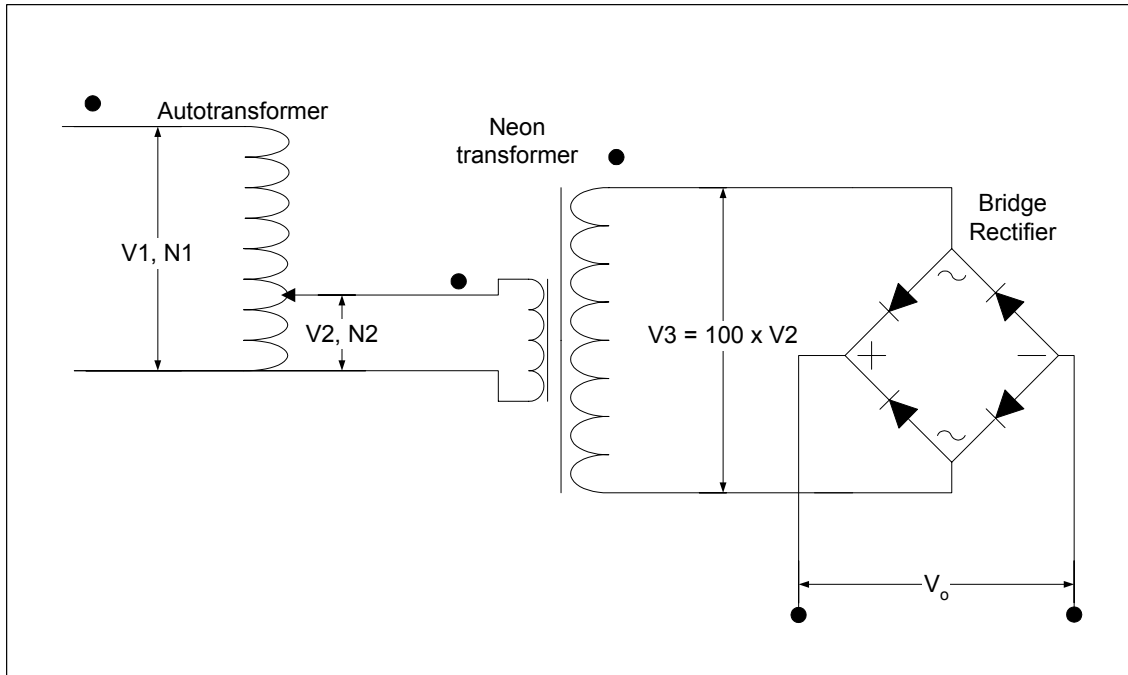


Figure 3.10: The neon transformer output connected to a bridge rectifier.

The output of the neon transformer is fed into the bridge rectifier configuration as shown. Theoretically, a maximum voltage of $\sqrt{2} \times 100 \times V_2$ can be expected on the rectifier output. V_2 is rms voltage at the output. The voltage across the output of the rectifier is give by

$$V_o = 100\sqrt{2}V_2 - V_{drop} \quad (3.14)$$

However, the voltage drop across the diodes V_{drop} will reduce the output by a small amount. The diodes used for the bridge rectifier in the power supply are rated at 125 kV PIV with 20 mA current. Each of the four sets used is a cascade of twenty one small diodes. The diode terminals and connectors have been covered with a thick layer of silicone sealant to prevent arcing or corona discharge. The voltage drop has been found to be 250 V.

3.6 The Capacitor

The simplest filter for a rectifier circuit is a capacitor. With the addition of the capacitor, the circuit is known as an unregulated linear power supply. The capacitor used for the power supply circuit has a rating of $1 \mu\text{F} \pm 10\%$ at 50 kVdc. The capacitor is large in size (22in x 8in x 5in, LxBxH) for a capacitance value of only $1 \mu\text{F}$ due to the high voltage withstanding capability. High voltage capacitors are bigger in size so that the dielectric medium separating the plates is thick enough to hold the increased potential.

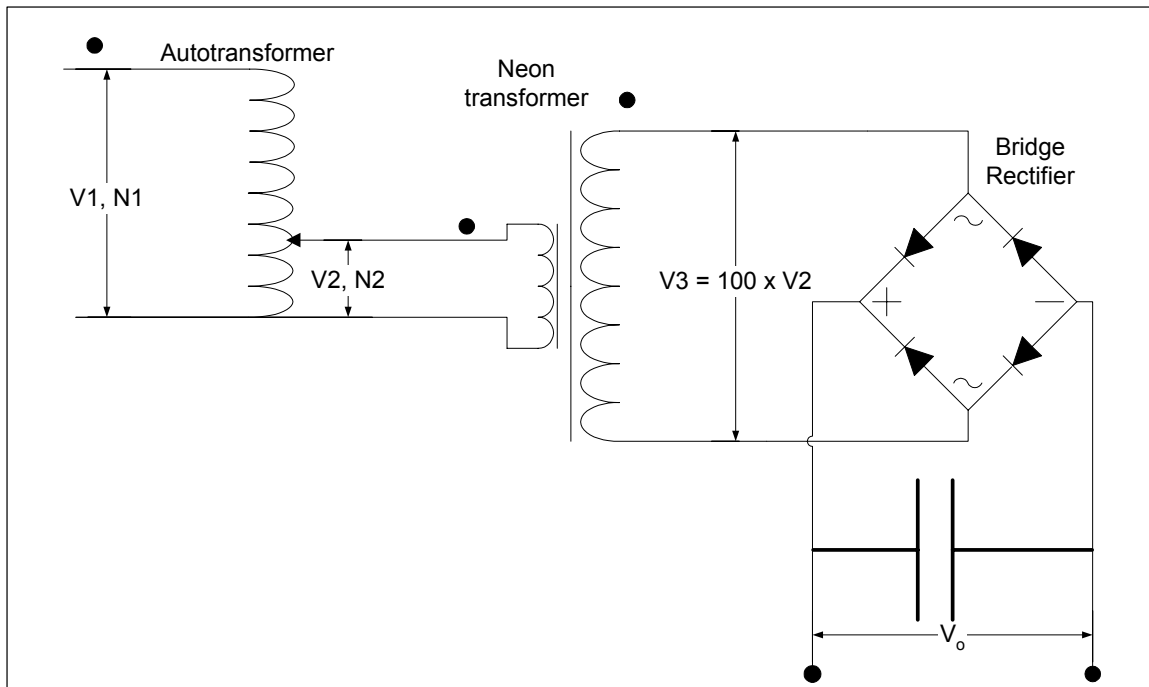


Figure 3.11: Rectifier with Capacitor filter.

The ripple factor for a capacitive filter can be found from the following equation, neglecting the diode voltage drops and a load resistance R_L connected across the capacitor. Here f is the frequency of the line voltage which is at 60 Hz.

$$RF = \sqrt{\left(\frac{V_{rms}}{V_{dc}}\right)^2} - 1 = \frac{1}{\sqrt{2}(4f R_L C - 1)} \quad (3.15)$$

For the test section, the corona discharge draws a current in the μA range, when a voltage in the order of 10^3 V is applied, which indicates a very high impedance in the order of 10^8 Ω . Thus, for an approximation, with the value of capacitance at 1 μF , the RF is found to be 2.95×10^{-5} , which is less than 0.3 %. This low value is because of the low current drawn. This is the reason why an inductive filter would not work. Inductive filters are for constant current loads, which is not the case for the test section. The test section is made of two electrodes separated by an air gap and it is essentially a capacitor. Therefore, it presents a high capacitive reactance to the current flow. Capacitive filters are simple yet effective for such a load.

3.7 The Power Relays

The output of the high voltage dc power supply is output through two sets of power relays, marked Re_1 and Re_2 in figure 3.12. These are fast switching high voltage electromechanically switching relays, able to switch on and off in 15 ms. These relays have a robust construction, with each device encased in a glass or ceramic container that is hermetically sealed and vacuumed.

Vacuum is the best insulator [32], because there are no atoms to conduct electricity. Vacuum can withstand an electric field density of 300 kV/cm while the dielectric strength of pure dry air breaks down at about 30 kV/cm. Therefore, the contacts of the relay can be very close to each other, allowing for very fast switching and small size. The contacts are also made of metals with high work function and

melting point. Metals with lower work function release electrons that can then exchange charge between the terminals of the relays at high potential. When a contact is broken by activating the relay, the current flow that was in the circuit tries to continue flowing and acts against the interruption forming an arc, just as the contacts are opening. This can heat up and vapourise the metal, leading to contact erosion. Thus these vacuum relays are made of low resistance copper alloys that can survive momentary heat.

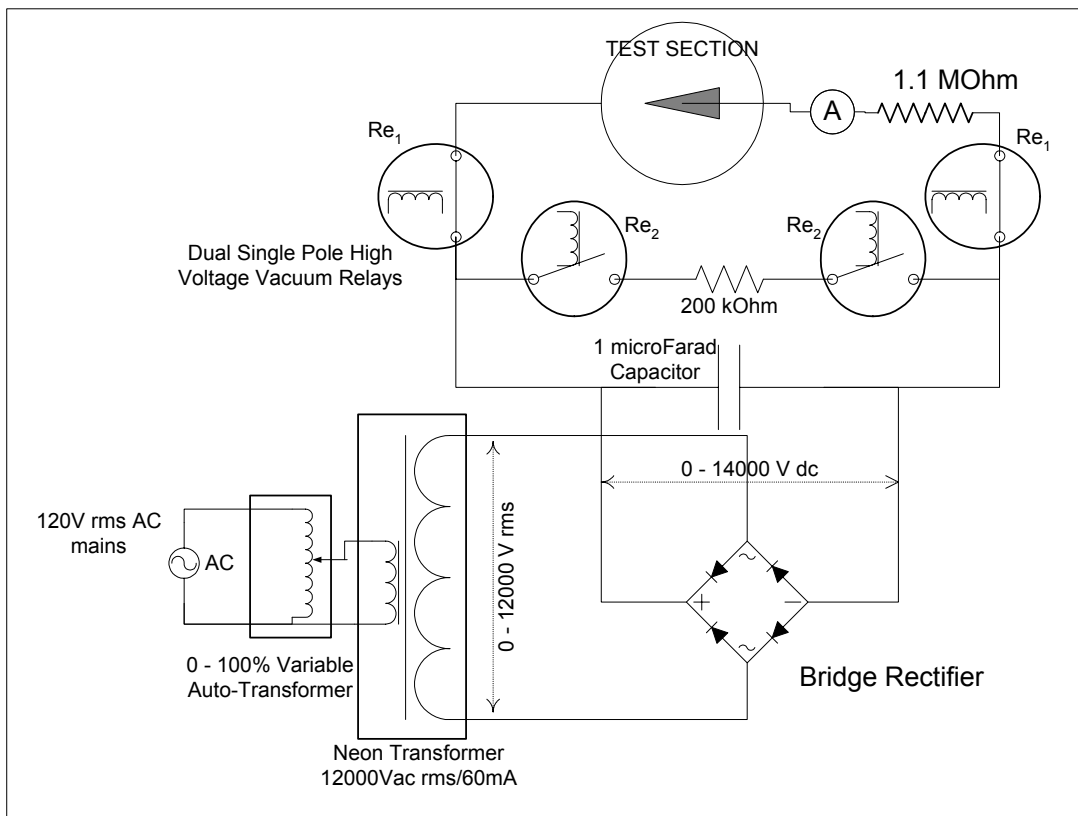


Figure 3.12: Power supply with the power relays at the output before the Test Section.

A mode of failure of relays is shorting to the metal housing of the relays' solenoid. This is why high voltage relays are made of ceramic, which has a very high dielectric strength able to withstand up to 250 kV/cm.

Vacuum relays are used in high frequency power switching applications, such as the high power supply to radio antennae. Microwave devices such as radars also use such relays to control the power to the radar antennae [33].

3.7.1 Electromechanical Relays vs. Solid State Switches

Solid state switches are semiconductor devices that can be used for very high voltage and current applications. They have the advantage of being very fast switching and are very robust. The fast switching speeds allow them to be easily integrated with digital control circuits, as their response times are similar, in the micro seconds range.

Most common used solid state switches are Silicon Controlled Rectifiers. They are similar to diodes in operation, allowing current flow in only one direction, but they also have a gate terminal, by which a small positive gate signal can be used to turn it on. However, once turned on, it does not turn off by itself. The process of turning off an SCR is called commutation, which often requires complicated circuits. The process by which the SCR is turned off by cutting off the load current is called load commutation. This is schematically represented in figure 3.13.

Another solid state device used for high voltage dc applications is a Gate-Turn-off Transistor (GTO), which can be turned off by a short negative pulse to the gate and does not require any commutation circuits.

The disadvantages of solid state switches are:

- They require commutation or turn off circuitry.
- They are very expensive.
- A big drawback to solid state devices is that they have a leakage current, both in

the forward and reverse biased condition. This is a small current that flows when the device is turned off and it is in the order of micro Amperes, which is the same order of the corona current.

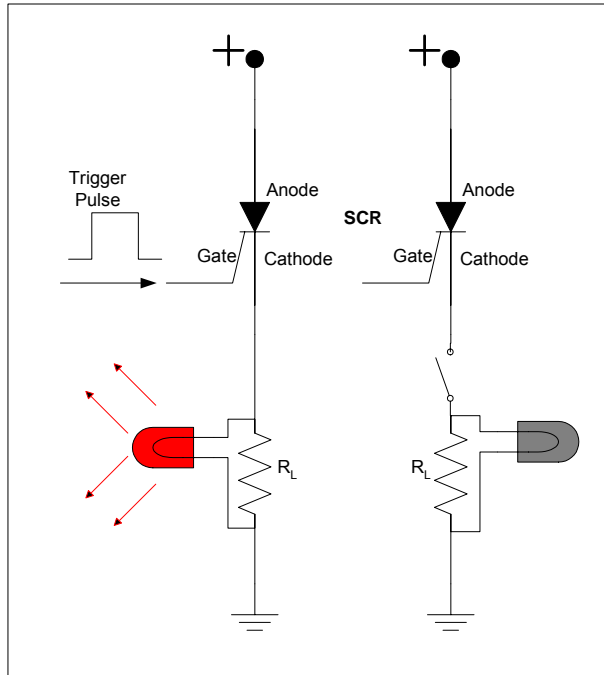


Figure 3.13: An SCR in the on mode (left) and Line commuted SCR (right).

Therefore, it was decided to use simple electromechanical vacuum relays for the switching. The response time of 15 to 20 ms was deemed to be acceptable for the experimental program.

3.7.2 Power Relays used in the Circuit

There are two types of power relays employed in the circuit. One is a pair of Single Pole Single Throw Normally Closed relays, white in colour; model number KC-32, shown as Re_1 in the figure 3.13, manufactured by Kilovac, CA, USA. [34] They are rated at 25 kV, 500 A peak, 45 A continuous. These are the relays that control the power to the load device, which is the test section. They operate on 12 Vdc. They are Normally Closed (NC) relays; therefore, they have to be energized to open the circuit.

The other pair of vacuum relays is the Russian made relays rated at 4kV nominal, 15 A continuous current and are green in colour. However, they can be used up to about 10 kV without breaking down. There are two of them in series, thereby increasing their voltage withstanding capability. These are used to discharge the capacitor through a total resistance of 1.3 M Ω . They operate on 24 Vdc.

3.8 DC Voltage Measurement

The voltage across the capacitor is measured as shown in figure 3.14. This is a voltage divider across the output capacitor, as shown, that amounts to 500 M Ω . The voltage is read across 5 M Ω resistance that yields a 1/100 voltage division.

The total resistances are made up of smaller resistors. Resistors also have a maximum voltage rating, beyond which their dielectric strengths break down or they conduct heavily and burn up. Therefore, resistors should be selected based on the highest voltage that they may encounter in the circuit. High voltage resistors are hard to find. Smaller resistors may be cascaded to achieve a higher voltage rating; however, they must be 'potted' in an insulating medium, such as insulating oil, asphalt, epoxy or silicon sealant.

The 500 M Ω resistance is composed of one 400 M Ω 1% precision resistor, one 80 500 M Ω 1% precision resistor and a series of 10 M Ω , 1%, 250 V, ¼ W resistors soldered together and then inserted into a plastic tube and then covered with silicon sealant. The 5 M Ω resistor is made by connecting two of the same 10 M Ω resistors in parallel. These are enclosed in a plastic enclosure by themselves properly sealed with silicon sealant. This box houses banana sockets that the voltmeter connects to. All the

wires are isolated and the probe cables going to the 5 MΩ box are isolated in a piece of foam pipe insulation.

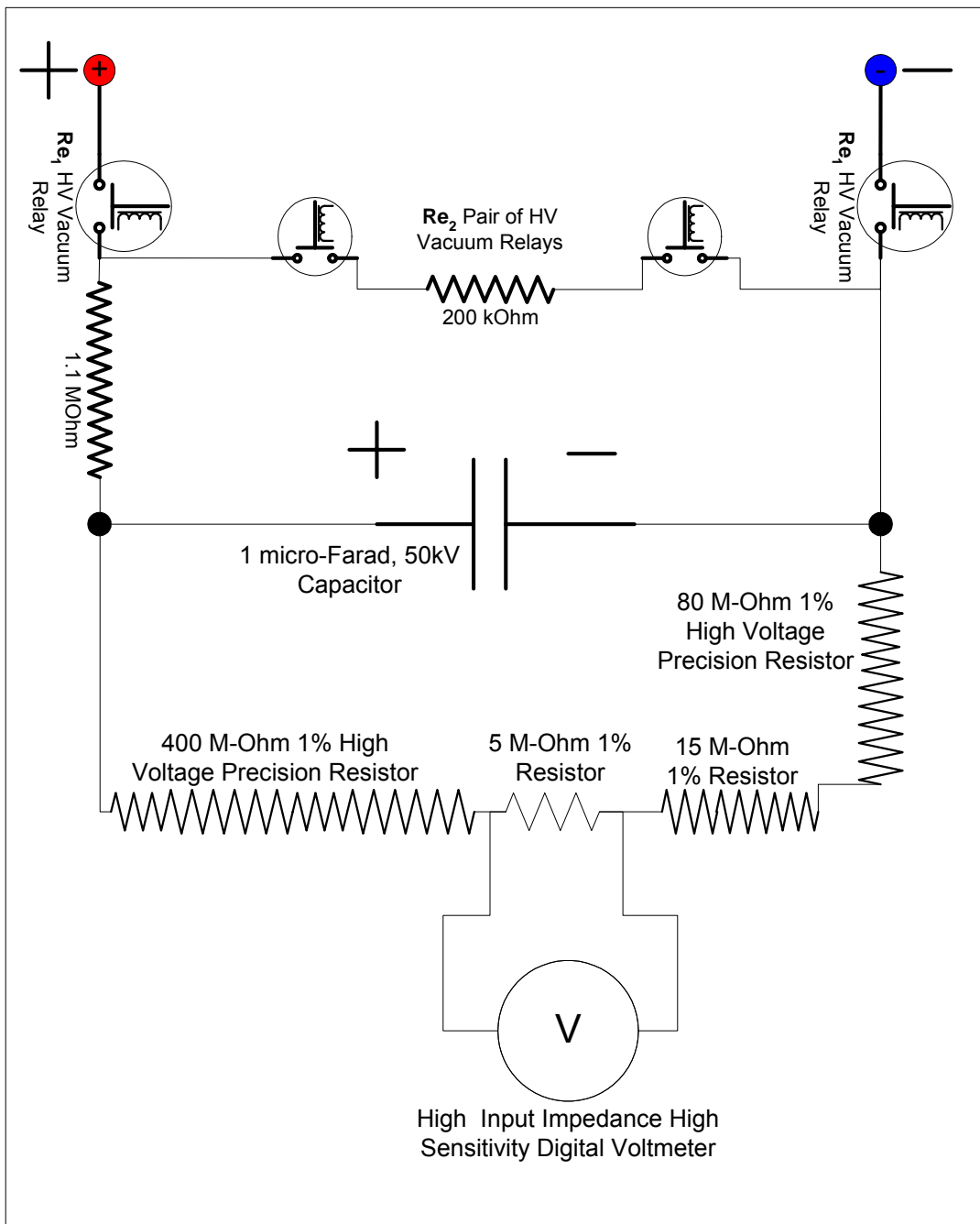


Figure 3.14: The voltage divider and digital voltmeter across the capacitor.

The voltmeter is a high input impedance digital meter; therefore it will not load the capacitor and cause a voltage drop. The model of the voltmeter used is Fluke 45 Digital Multimeter, rated at 650 Vdc, 250 mA.

The measurement of the final voltage output by the power supply is not affected by the accuracies of the individual components. The use of high precision 1% tolerance resistors in the voltage divider circuit and a high accuracy digital voltmeter guarantees that only the uncertainties of these devices need to be considered for the voltage measurement.

If V_o is the voltage across the capacitor, the reading on the voltmeter V_r is given by

$$V_r = \frac{1}{100} V_o \quad (3.16)$$

$$\therefore V_o = 100 V_r \pm 1.41\% \quad (3.17)$$

The uncertainty of the voltage reading has been calculated to be 1.41 % of the voltmeter reading.

Another feature to be noted here is that the voltage divider drains current from the capacitor. Thus if the HV AC is cut off to the capacitor, it will eventually drain out. The time constant of the RC circuit is very large, equal to 500 seconds.

$$R C = 500 \text{ M}\Omega \times 1 \text{ }\mu\text{F} = 500 \text{ seconds.} \quad (3.18)$$

In 500 seconds, the capacitor loses 63.2 % of its original voltage. Therefore, it allows for the capacitor to hold a steady voltage for a significantly long time after the ac power has been turned off [35].

3.9 The Control Box

The control box has a built in power supply that delivers power to the power relays across the power capacitor. The heart of the control box power supply is a 120 V to 24/12 V step down transformer. Bridge rectifier modules are used to convert to three dc voltage outputs, namely two 12 Vdc and one 24 Vdc. The power supply has its own cooling fan. The main switch is located at the back of the control box. The front panel of the box has 3 toggle switches and 4 light emitting diodes (LED) that indicate the state of the relays and the power supply.

On the back panel are the mated connectors that only accept the specific type of connectors, so that no mismatched connections are possible. One two-conductor connector is for the High Voltage AC Power Supply. Another four-conductor connector links to the Power Relay box, which has two types of relays: one pair for the power output and one pair for the capacitor discharge.

When the main switch is turned on, a red LED lights up indicating that AC power to the transformer is turned on. The cooling fan also turns on simultaneously. The three toggle switches are of different types, each controlling a different type of relay. One toggle switch is marked HV AC P/S, standing for High Voltage Alternating Current Power Supply. This is a SPST switch. The second toggle switch is marked O/P RELAY CLOSE. This is a DPDT switch. The third toggle switch is marked CAPACITOR DISCHARGE and it is a SPST spring return switch.

When the toggle switch marked HV AC P/S is put to the “ON” position, the red LED above it turns on indicating that ac power to the neon transformer is now turned

on. The power output relays, the white Kilovac relays, are NC relays. Therefore, when the control box power supply is turned on, with the toggle switch marked O/P RELAY CLOSE in the off position, the white relays are energized and their contacts are opened and the green LED above it will be off. When this toggle switch is put to the “ON” position, the LED comes on and the white relay contacts are closed. (The relays are now de-energized.)

The third toggle switch is used to discharge the capacitor. It has two positions. When pushed up, it latches to the “ON” position and the yellow LED above it comes on, indicating that the green relays are energized and their contacts are closed. When it is pushed downward, it will light up the yellow LED, indicating the green relays are energized, but the switch will go back to the off position when released. This feature is for momentary discharging of the capacitor, for example to bring down the voltage in the capacitor momentarily.

The function of the control box is to give the user the ability to control the high voltage ac generator and the output relays from a remote location, for example where the data measurement devices are located or inside the control room away from the high voltage equipment. The cables linking the control box to the specific components are easy to extend and thus the control box can be practically located any where in the lab. This makes the power supply very versatile.

The detailed circuit diagram of the control box is shown in the appendix. The following figure shows the layout of the front and rear panels of the control box.

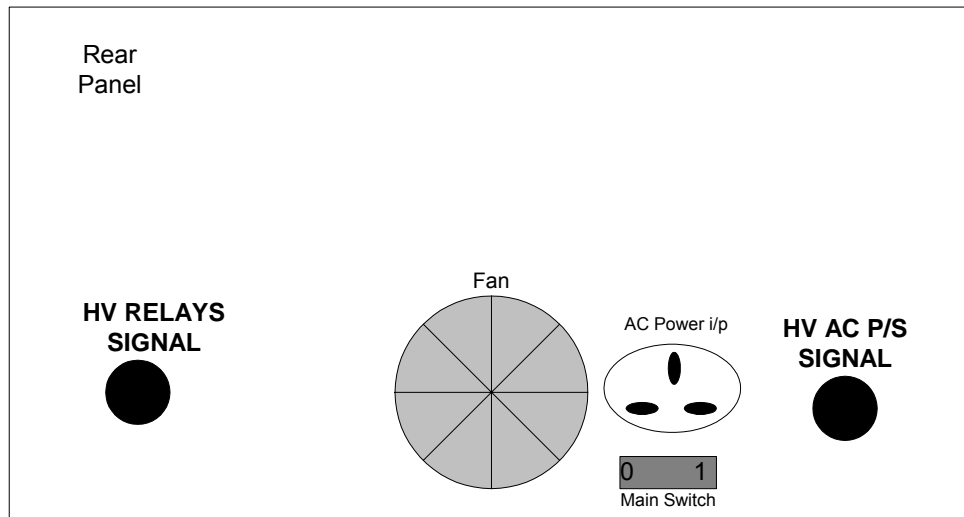
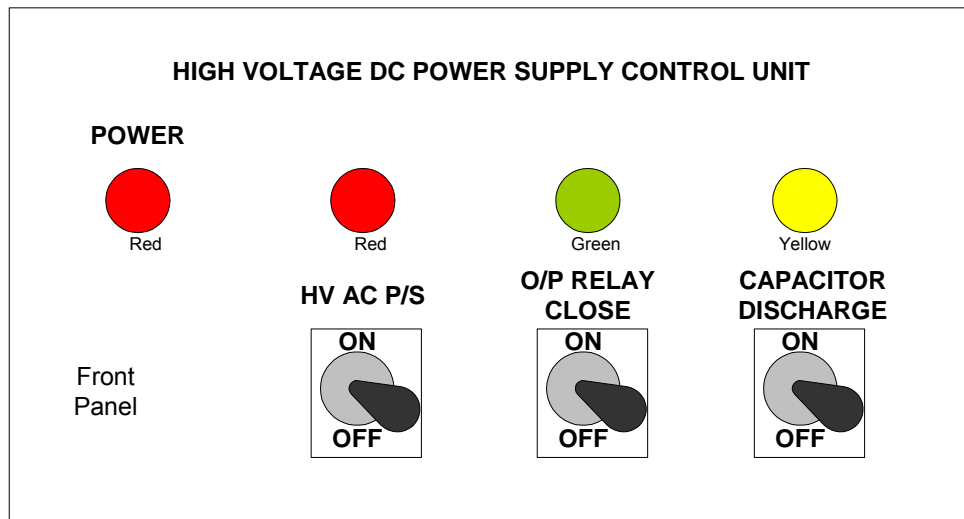


Figure 3.15: The front and rear panels of the Control Box.

3.10 Features of the High Voltage Power Supply

The High Voltage DC Power Supply is built as smaller modules that are housed in separate boxes. This serves several purposes. It helps in electrically isolating the high voltage components from the low voltage ones. It makes it easy to locate, identify and access parts of the circuit.

Shown in figure 3.16 below is the layout of the power supply.

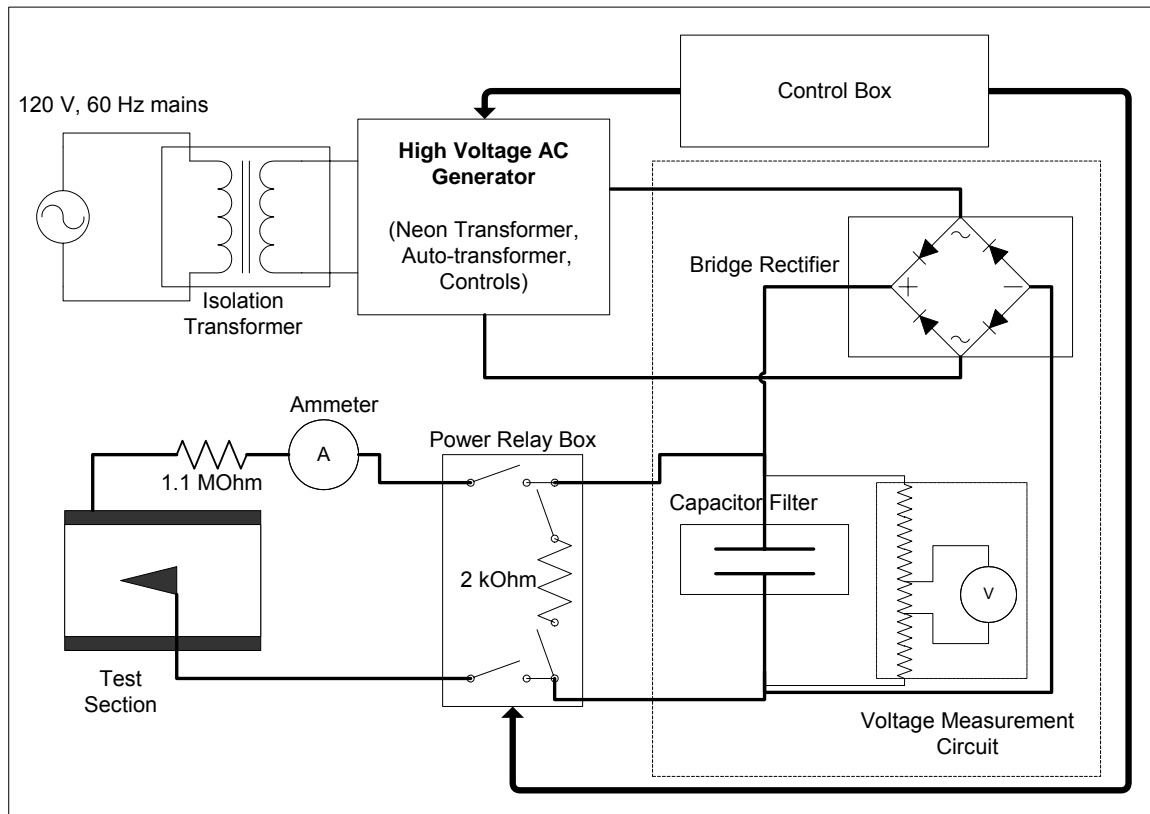


Figure 3.16: Schematic of the power supply

The different modules of the power supply are:

- High Voltage AC Generator (HVACG)
- Rectifier
- Capacitor
- High Voltage Measurement Circuit
- Relay Box including Capacitor Discharge Resistor
- Current Limiting Resistors
- Current Measurement Circuit
- Control Box

The High Voltage AC Generator (HVACG): The HVACG is housed in a wooden box. The HVACG contains the variable auto-transformer, the neon transformer and control circuits. The top panel of the HVACG is shown in figure 3.17. This module plugs into the domestic ac mains. The ac power for the control circuit of the module is separated from the high voltage power side of the circuit and their connection sockets are located on either side of the box, as seen in the figure. The high voltage side is supplied through a large isolation transformer to protect the ac lines of the building from any high voltage leakage back into the line.

Both sides have panel mounted line filters; the high voltage side filter has dual 6.3 A fuses. The line filters are low pass filters that allow 0 to 400 Hz signals through, while attenuating higher frequency signals and transients. They work in both directions, stopping noise from line to the equipment and noise from the equipment to the line [36].

When the power cables from both sides are connected to the mains, two red LEDs marked TRANS PWR (transformer power) and CNTRL PWR (control power) lights up on the LED panel on the top of the box. This shows that the fuses in the ac line filter or the filters themselves are functioning properly.

When the main switch is turned on, the yellow LED marked MAINS turns on. However, the power has not reached the transformer yet. The SPDT toggle switch next to the main switch has to be set to the appropriate position for power to be supplied to the transformers. In the LOCAL ON position, the SPDT relay controlling the power to the transformer is turned on. In the REMOTE position, the signal from the control box is required to turn on the relay. The remote control cable is plugged into the banana

plug sockets below this toggle switch. (The colour coding of the cable should be noted; the red and black connectors should be plugged into their respective colours only, otherwise the SCR in the Control Box will not trigger properly and the red LED marked HV AC P/S on the Control Box front panel will not light up.)

When the relay is on, the green LED marked POWER O/P lights up. Now the transformers are receiving power and the output of the HVACG is supplying a high voltage depending on the auto-transformer position.

The auto-transformer knob is located to the left of the LED panel. It can be set at a desirable location to get the required output voltage. The knob position should be set while reading the Voltmeter across the capacitor.

The SPDT toggle switch marked VOLTMETER READING is for controlling the input to the analogue ac voltmeter on the panel. When it is set to SUPPLY POWER the voltmeter reads the mains power supply. When set to I/P POWER, it reads the output of the autotransformer, which is the input to the neon transformer. The HVACG output is now 100 times the reading on the voltmeter. (Note that the voltmeter reads RMS value. Therefore, the dc value will be much higher.)

The design of the HVACG is such the neon transformer can be easily changed for a different secondary voltage and VA rating to get higher or lower dc voltage output and current capacity. The diodes in the rectifier have a PIV of 120 kV, so that any rating of neon transformer can be safely used in the circuit. Thus a 12 kV, 720 VA transformer will deliver a maximum dc voltage of about 16 kV and a maximum possible current flow of 60 mA, after the voltage drop across the diodes have been taken into account. If

a higher voltage is required, the next available step in the neon transformer secondary voltage rating is 15 kV, which can potentially deliver a dc voltage of about 21 kV. Since the neon transformers are poorly regulated, a different type of high voltage step up transformer can be substituted safely if available.

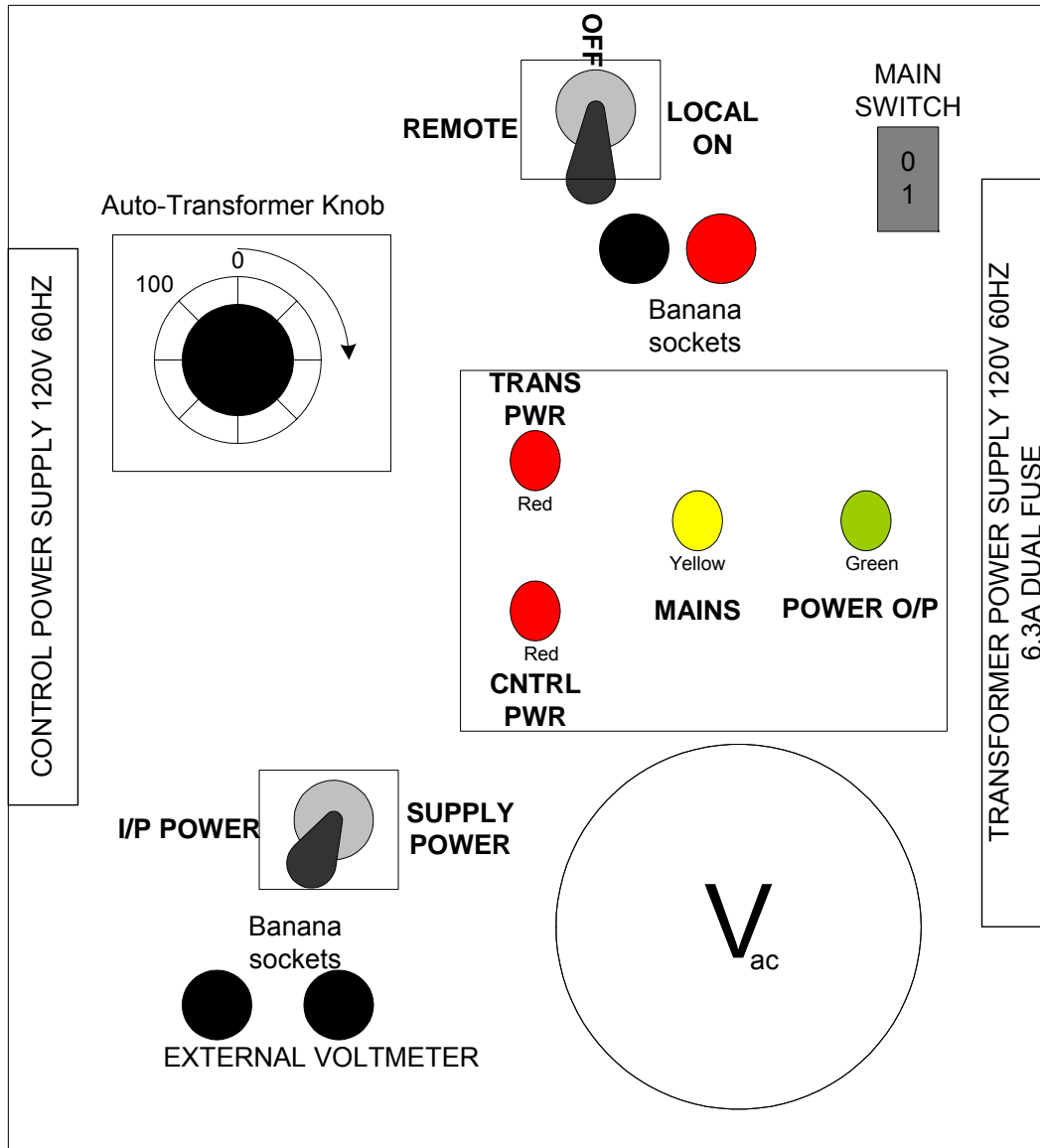


Figure 3.17: Schematic of the High Voltage AC Power Supply's Top Panel.

The rectifier assembly is housed in a Plexiglas box. The connecting cables are bolted on to terminals extending through the walls. The output of the rectifier goes to the capacitor, which is also housed in a Plexiglas box. The voltage measurement circuit is composed of the high voltage resistors and the digital voltmeter. The rectifier, the capacitor and the high voltage measurement devices are mounted on a cart, so that it can be easily moved. The output of the capacitor is connected to the Relay Box.

All connecting cables in the high voltage side of the circuit are made of high current 22 AWG (7/30) copper braided wire, that have insulation rated at 10 kVdc and temperature rating of 150°C. In addition, the cables have been covered with ½ inch thick foam pipe insulation used for thermally insulating air conditioning copper pipes and then taped over with one layer of duct tape and a layer of electrical insulation tape. Therefore, the wires are extremely well insulated. The insulation tape also serves as colour coding, with the different cables covered in tapes of black, blue and red colours, for easy identification.

The Relay Box houses the pair of white Kilovac Power relays and the pair of green Russian capacitor discharge relays. The cables from the capacitor are bolted to connectors on one side of the box. The output is made available through recessed high power sockets that only accept specific sized connectors. These allow for easy plugging in or removal. The polarity of the output power is thus changed by plugging the connectors of the load into the positive and negative sockets as required.

3.10.1 Current Limiting and Capacitor Discharging Resistors

As mentioned earlier, when the ac power to the capacitor is cut off, the 500 MΩ

resistors will drain the capacitor slowly. A quicker discharge is made possible through a set of high power resistors. The resistors are composed of 100 kΩ ±5%, 20 W resistors, connected in series to total 1.3 MΩ. These resistors are connected in two sets of 1.1 MΩ and 2 kΩ, as shown in figure 3.18. The 1.1 MΩ resistance is for current limiting. Thus, at a maximum dc voltage of 15 kV, if the output terminals were shorted, the maximum possible current flow is set as

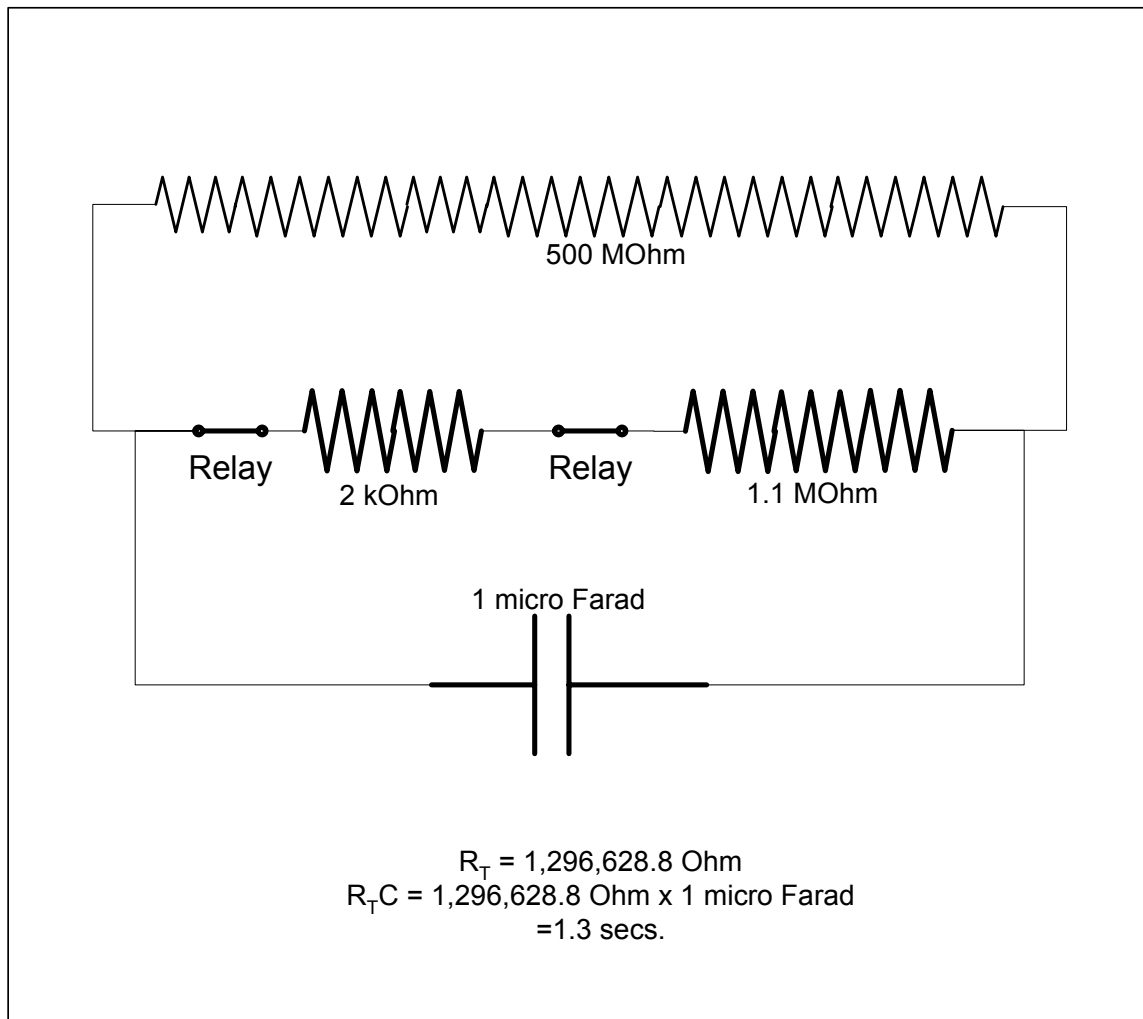
$$i_{\max} = \frac{V_{\max}}{R} = \frac{15000V}{1.1M\Omega} = 13.64mA \quad (3.18)$$

This prevents arcing. The resistors have been selected based on power consumed during maximum current flow, rounded off to 14 mA. The calculated power for each resistor is found to be 19.6 W.

$$P = I^2 R = (14mA)^2 100k\Omega = 19.6W \quad (3.19)$$

Each resistor has a value of 100 kΩ, 20 W, and they can withstand brief inrush currents much higher than 25 mA without burning up. However, during normal operations, these current limiting resistors will result in a voltage drop across them. It was experimentally that the current flow during corona discharge is in the μA range. Therefore, for a maximum corona current at a safe level of 50 μA, the voltage drop across the 1.1 MΩ resistors is

$$V_{drop} = I_{corona} R = 50\mu A \times 1.1M\Omega = 55V \quad (3.20)$$



This is a small price to pay for a good level of safety. During normal operations, the voltage drop across the resistors has to be deducted from the voltmeter reading to get the voltage applied across the test section.

Figure 3.18: Circuit showing the current limiting, capacitor discharging and voltage measurement resistors.

For discharging the capacitor, the green relays have to be closed. Thus the 2 kΩ resistors in the relay box in between the pair of green relays come in series with the 1.1 MΩ resistors, totalling 1.3 MΩ. This resistance forms a parallel resistor network as

shown in the diagram above. Thus the equivalent resistance is found to be 1.297 M Ω .

Now the capacitor discharges quickly, as the time constant drops to 1.297 seconds. The capacitor will discharge to a safe level (less than 50V) in about 15 seconds.

3.11 Current Measurement of the High Voltage DC Output

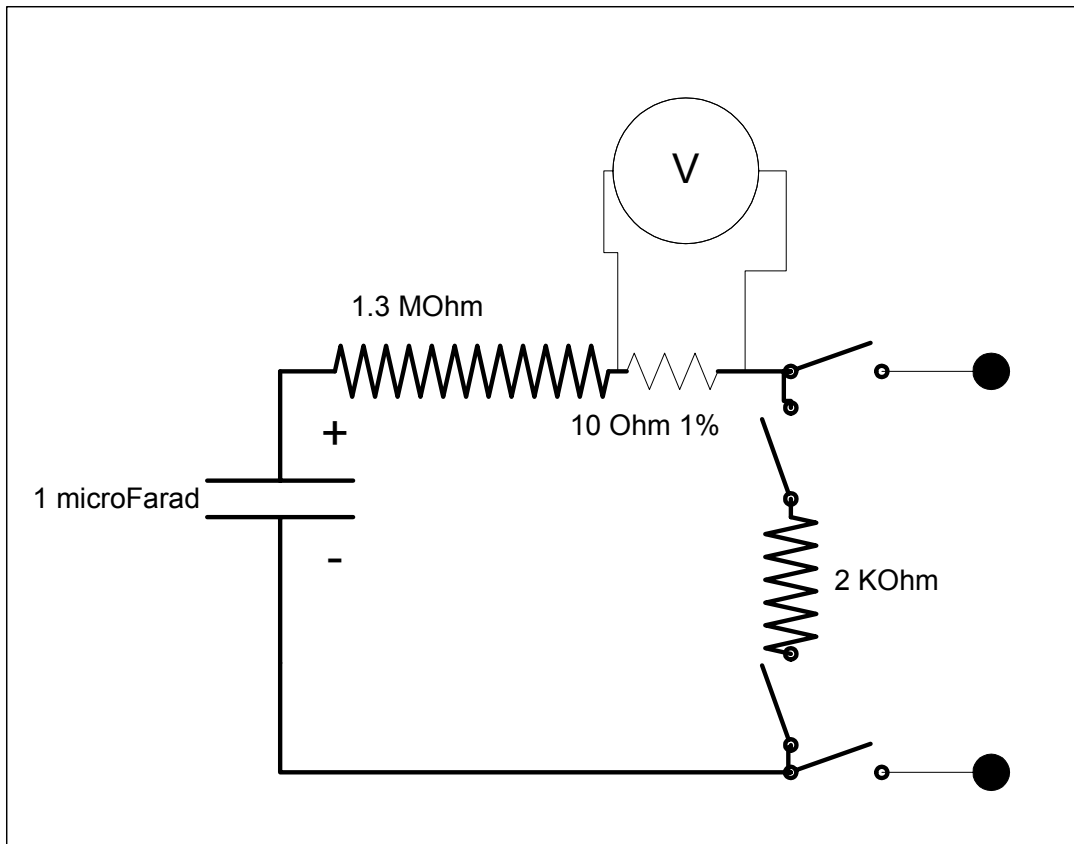


Figure 3.19: Current measurement circuit.

The current flow in the output is measured by a voltmeter reading the voltage across a $10\ \Omega$ 1% $\frac{1}{4}$ W resistor. The voltmeter is a high input impedance digital HP 3468A voltmeter. The current is obtained by directly dividing the reading on the voltmeter by 10.

$$i = \frac{V_{\text{reading}}}{10\ \Omega} \quad (3.21)$$

The uncertainty in the measurement of current with this circuit has been calculated at

1%. The HP 3468A digital multimeter is capable of reading as low as 1 μ V and as high as 300 Vdc.

3.12 Safety Features of the High Voltage DC Power Supply

The safety features incorporated into the design of the High Voltage DC Power Supply are listed below.

- The power supply to the high voltage side of the HVACG, containing the neon transformer, is supplied through a 1 kVA Line Noise Suppressing Isolation Transformer, that prevents line noise from getting to the HVACG and high voltage leaks from getting back into the supply line.
- There are separate lines for the high voltage side and the low voltage control circuits in the HVACG.
- Each supply line to the HVACG has a Line Filter. Line Filters protect the equipment from line noise and stop transients from the equipment from going back into the line.
- The Line Filter on the high voltage side holds two 6.3 A fuses, that protect the circuit from over currents.
- There is a fuse in line with the input to the auto-transformer. Thus two levels of fuse protection are present in the circuit of the HVACG.
- Neon transformers have a built in safety feature of current limiting. The iron core of the transformer saturates if the secondaries are shorted (as in the case of an arc across the rectified output), whereby an increase in current flow beyond about 1.1 x the rated maximum current is not possible.

- The capacitor is drained by the high voltage resistors of the voltage divider network, used for measuring the voltage across the capacitor. However, this takes about 30 minutes for the voltage to drop to a safe handling level. This is only a safety feature if the capacitor is not discharged.
- There is a capacitor discharge circuit set up to discharge the capacitor down to a safe level (<50V) in about 10 seconds.
- The current is limited to a maximum of 14 mA by a current limiting resistor. This prevents arcing at the output. However, this current at higher voltages can still cause spark discharges to occur.
- The cables connecting the high voltage side of the circuit are all rated at 10 kVdc and then covered with ½ inch thick foam pipe insulation and tightly taped over with electrical insulation tape.

3.12 Drawbacks of the High Voltage DC Power Supply

The Power Supply is unregulated. Therefore, as more current is drawn, the voltage across the output falls. At regular corona discharge currents the voltage drop is not significant and can be compensated by increasing the voltage output with the auto-transformer until the required voltage is reached. What this does is to increase the input to the neon transformer, thereby increasing the output of the transformer and the corresponding rectified output. This is a dynamic compensation method. The reason for the poor regulation is two fold. One reason is the neon transformer itself because neon transformers are designed with poor regulation, as that is how neon tubes work. As the neon gas in the tubes gets ionized, they draw more current, therefore, they require less

voltage. This works well for neon light applications. Also the current limiting feature of the neon transformer affects the secondary winding output regulation, as the windings are loosely coupled with the core. The second reason for poor regulation of the power supply is that components required for constructing regulator circuits, such as inductors and semiconductor devices are not easily available with high voltage ratings and are very expensive. Therefore it would be very expensive to fit a voltage regulator circuit to the power supply. Ripple in the circuit is present, although highly attenuated, but as current flow increases the ripple factor increases. It is difficult to completely eliminate ripple, but to further minimize ripple, more capacitors would be required. Filter circuits for high voltage levels are not easy to build because of the difficulty in procuring components rated at high voltages. The relays do have a small capacitance value. This allows a 60 Hz signal to pass through to the output even when the contacts are open. This does not affect the dc operation of the circuit. Despite its drawbacks, the High Voltage DC Power Supply performs quite well and it meets the power requirements for the corona discharge project.

3.14 Operation of the High Voltage DC Power Supply

1. Before operating the power supply, ensure that the circuit is complete and there are no unconnected or loosely connected cables.
2. Connect the control box to the remote control sockets of the High Voltage AC Power Supply Generator (HVACG) Box with the right cable, making sure the polarity of the banana plugs are matched (red to red and black to black).
3. Connect the control box to the relay box with the right cable. Make sure all the

toggle switches on the front panel are in the off position.

4. Turn on the Fluke 45 multimeter to read the output of the capacitor. Also turn on the HP 3468 multimeter to read the current flow.
5. Turn on the Control Box main switch located at the rear. The white Kilovac relays should open as it is turned on. The relays make an audible sound. The cooling fan at the rear of the Control Box should turn on. The red LED marked POWER on the front panel of the Control Box should light up.
6. On the HVACG box, set the toggle switch next to the main switch to the OFF position. Connect the two power cables of the HVACG to the mains. Make sure the cable to the high voltage side, labelled TRANSFORMER POWER SUPPLY 120V 60HZ 6.3A DUAL FUSE, is connected to the mains through the 1 kVA Isolation Transformer. Two red LEDs on the top panel of the HVACG marked TRANS PWR and CNTRL PWR should light up. If they do not, it suggests that the fuses on the transformer side are blown or the line filters are malfunctioning. If the LEDs light up, further operations are possible. If not, the issues have to be resolved.
7. If the LEDs are lighted, turn on the MAIN SWITCH. The yellow LED marked MAINS should now light up. If not, the fuse in line could have been blown.
8. Set the toggle switch labelled VOLTMETER READING to SUPPLY POWER and observe the analogue ac voltmeter reading. It should read about 120 V, showing the voltage of the mains supply. The other position of the toggle switch labelled I/P POWER allows the voltmeter to read the input to the neon

transformer. The rms voltage output of the neon transformer will be 100 times this reading, if it is a 12000 V neon transformer.

9. The toggle switch next to the main switch may be set to LOCAL ON and the control box control will be overridden. Set the toggle switch to REMOTE to control the HVACG from the control box.
10. On the control box, turn on the toggle switch labelled HV AC P/S. The red LED above the switch on the control box should now turn on. On the HVACG top panel, the green LED labelled POWER O/P should be lit as well.
11. Now the HVACG is supplying high voltage. Rotate the knob of the auto-transformer on the HVACG clockwise to increase the voltage and counter clockwise to decrease the voltage. Observe the reading of the voltmeter on the capacitor as the knob is rotated. The actual voltage across the capacitor is 100 times the reading. When a reading just below the required voltage is reached, stop turning the knob; wait for the voltmeter reading to stabilize and then make the finer adjustments on the knob. It takes a few seconds for the reading to stabilize. If the capacitor overshoots the required voltage, the capacitor can be momentarily discharged or brought low by pressing the toggle switch on the control box marked CAPACITOR DISCHARGE downward. It has a spring return and will reset to the off position when released. The yellow LED above the toggle switch should light up during the discharge process.
12. Once the required voltage is reached, on the control box, turn on the toggle switch marked O/P RELAY CLOSE. The green LED above the switch should

- light up. The relay contacts are now closed and the capacitor output is being applied across the load.
13. Note the current reading. The current reading is the reading of the hp digital Multimeter, (set to dc volts), divided by 10.
 14. The actual voltage across the load has to be determined by finding the voltage drop across the current limiting resistors, which is $1.1 \text{ M}\Omega \times$ the current flow. The resistors have 5% tolerance.
 15. To turn off the high voltage dc power output, turn off the toggle switch marked O/P RELAY CLOSE.
 16. Cut off power to the neon transformer in the HVACG by setting the toggle switch marked HV AC P/S to the off position.
 17. Discharge the capacitor by turning on the toggle switch marked CAPACITOR DISCHARGE to the on position. The yellow LED should light up. Once the capacitor is discharged to a safe level, observed by the reading on the voltmeter, the circuit is safe to handle.
 18. Turn off the HVACG by turning off the Main Switch.
 19. Once the experiment is over, remove the cables to the HVACG. Turn off the control box main switch. Turn off the voltmeters finally once it is ascertained that there is no high voltage on the capacitor. The reading of the capacitor will fluctuate within a positive and negative low mV reading. This is due to the resonance in the circuit due to the capacitor, the capacitance and inductances of the wires, resistors and other components.

CHAPTER IV

THE CORONA DISCHARGE TEST SECTION

4.1 Features of the Design

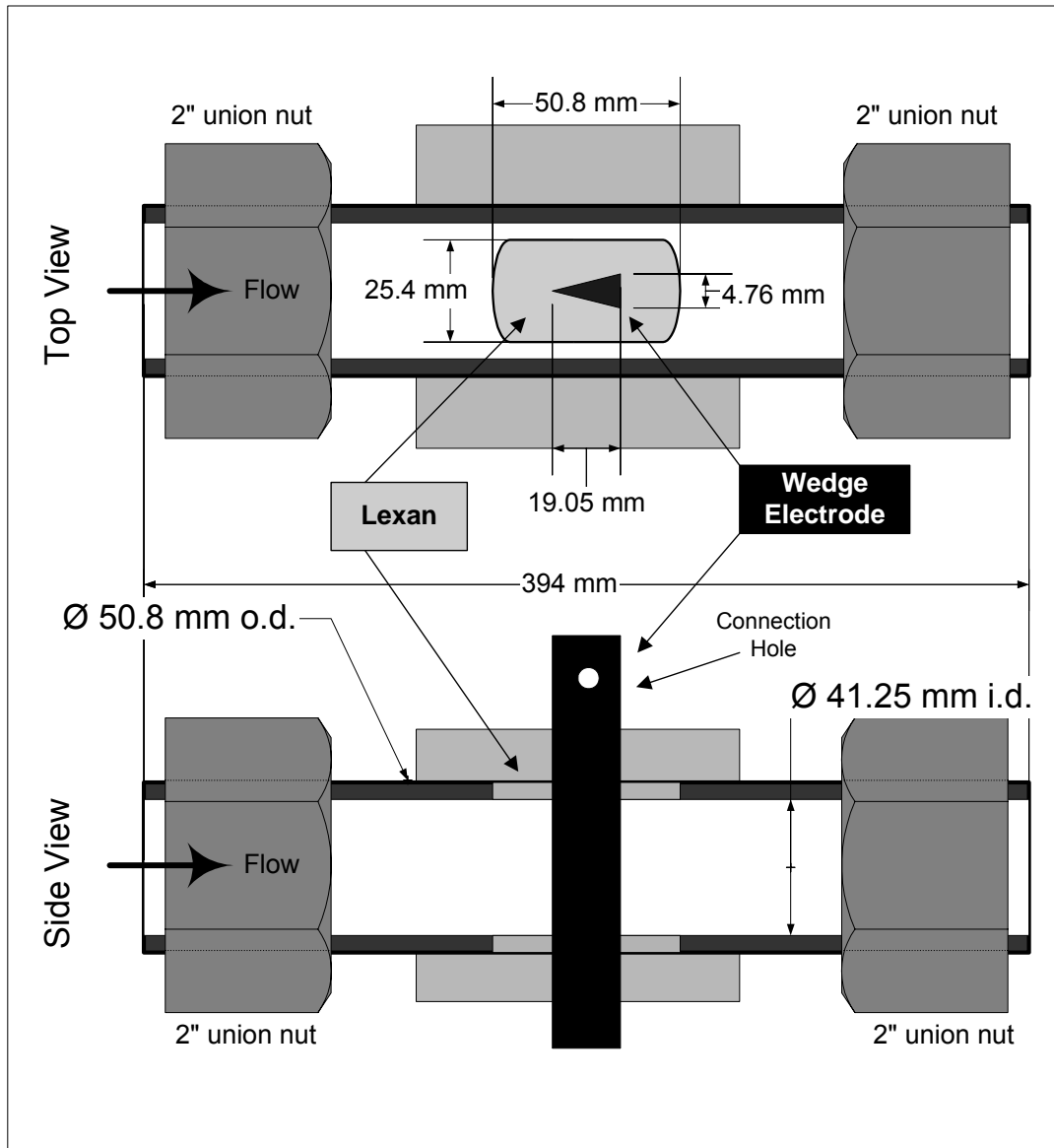


Figure 4.1: Top and side view of the test section.

The test section is constructed on a piece of 304 stainless steel tube 394 mm (15.5 in.) long and 50.8 mm (2 in.) outer diameter. The inner diameter is 41.25 mm (1 5/8 in.). Close to the middle of the tube, a cavity is cut into the tube as shown in figure 4.1 above. Into this orifice, a triangular wedge, made of 316 stainless steel, is inserted and rigidly held in place by Lexan [8] blocks that are machined to press fit onto the assembly such that the interior is cylindrical and the inside surface is flush with the inside surface of the steel tube. The reasoning for this design includes mechanical and electrical aspects.

4.1.1 Mechanical aspects of this design

The test section has to fit into the shock tube, as explained before, for the second phase of the study involving supersonic tests. Therefore, the construction is made of materials that can withstand the huge forces developed during the operation of the tube. The wedge and the steel tube are joined together by machined blocks of Lexan. Lexan has high tensile strength, is highly impact resistant and can withstand heat up to about 150°C. It is also relatively easy to machine. Lexan is translucent.

The stainless steel tube is the same size as the shock tube. This is why the test section has 2 inch union nuts attached to it, so that it can be screwed onto the 2 inch union connectors on the shock tube.

The wedge shape has been adopted for its advantageous aerodynamic qualities. In a supersonic flow, a sharp triangular wedge presents a lower profile than a blunt body, resulting in a weak attached shock formation, whereas a blunt body creates a strong bow shock. The pressure losses due to the attached shocks are lower. Thus the

wedge results in a smaller aerodynamic loading than a blunt object with the same cross section. The force felt on the wedge is also transmitted to the Lexan blocks that can cause shear damage in the Lexan. Therefore, the wedge would be preferable to a blunt body.

Behind the wedge, a wake occurs in the flow. This feature can be exploited in a supersonic engine, where the circulation can perhaps help in better air-fuel mixing.

4.1.2 Electrical aspects of this Design

The wedge and tube are the two electrodes, with the wedge being the active electrode and the tube body being the passive electrode. The electric field strength around sharp and pointed objects, like the wedge, is higher than the flatter surface of the tube. The sharp edge and the sides of the wedge provide more high-potential surface areas to ionize the gas flowing past them.

Thin wire electrodes are inappropriate in a supersonic flow, as it will result in a bow shock formation in front of the wire and face a more severe force from the flow. This can lead to the wire being deformed or broken. Breakage of the wire while the high voltage dc is applied can cause shorting of the output, resulting in arcing, thus causing more damage to the electrodes.

However, in the present design, the closest location of the wedge to the tube body is at the back of the wedge, where the separation from the tube is about 1cm. This is where the likelihood of arcing or sparking occurring is greatest.

Lexan is a good insulator of electricity with a dielectric strength of 15 kV/mm. It is a flame retardant material. Still, Lexan has poor resistance to solvents such as

Acetone. Also Lexan tends to carbonize when arcing occurs over its surface. Carbon conducts electricity and therefore, carbon deposition on the surface defeats the purpose of Lexan as an insulator.

A major problem with the manufacturing of the test section is that the surface of the Lexan on the inside of the pipe is not exactly flush with the surface of the steel pipe, as shown in figure 4.2. The Lexan is about 0.5 to 1 mm below the steel surface. This makes the edges of the raised portion of the steel tube to appear as sharp surfaces, causing the electric field strengths around them to be very high. Thus arcing can be induced between these edges and the wedge. It is recommended that this depression be filled with an insulating heat resistant material.

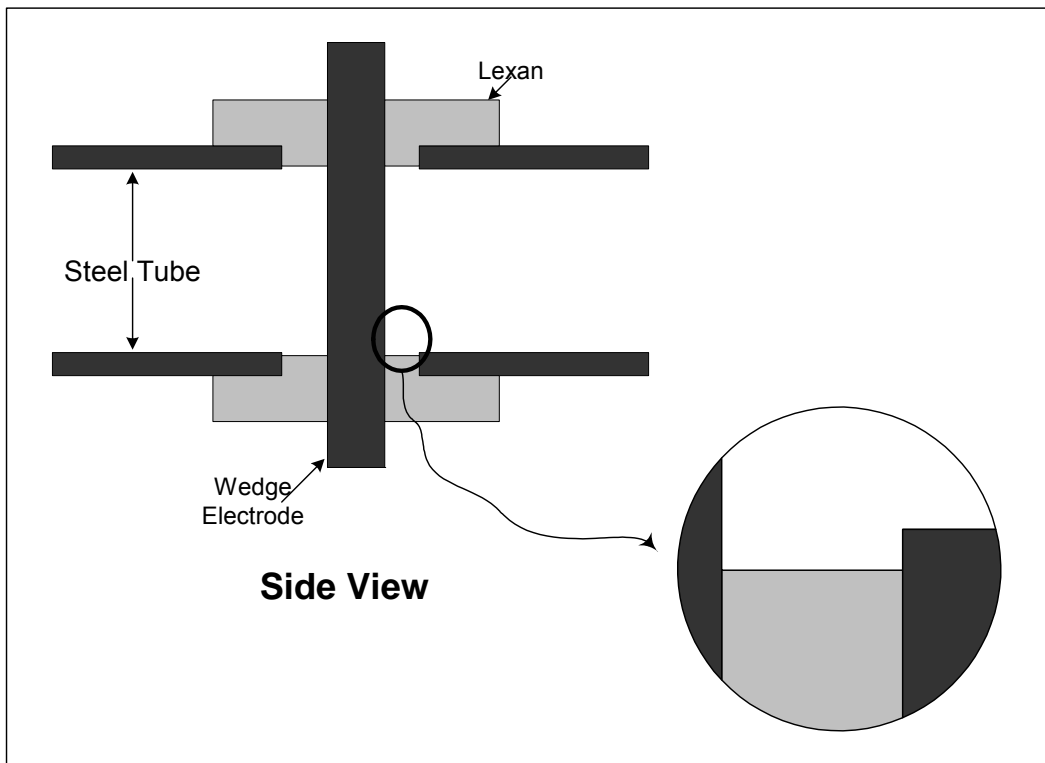


Figure 4.2: A side view showing the imperfection in level of the Lexan and the steel surfaces.

A better material in place of Lexan would be ceramic. Ceramic has dielectric strengths of about 250 kV/mm, can withstand very high temperatures, and has high strength and good resistance to chemical solvents. However, it is brittle and will have to be reinforced with some external structures and ceramic is hard to machine and cut. The ceramic parts may have to be moulded. This can increase costs.

The electrical lead is bolted to the wedge through a $\frac{1}{4}$ inch hole drilled through it at the top. The wires are insulated with the foam pipe insulation and taped. The joint of the wire and the part of the wedge protruding outside the Lexan blocks are also covered with silicon sealant to prevent any corona discharge on the outside of the test section. The electrical cable from the wedge is covered with black and red insulation tape and the cable from the tube is covered with blue tape, for easy identification. The Lexan blocks are held in place by a system of clamps which are fastened with bolts and nuts.

CHAPTER V

ION DETECTION PROBES

Plasma is a conducting gas composed of charged particles, ions and electrons. Neutral plasma has an equal number of negative and positive charged particles. For most applications involving low temperature and low kinetic energy plasma, the Maxwell distribution of particles is adopted [14]. The Maxwell distribution is based on the velocities of the particles. The mean kinetic energy of a particle in 3D space is shown as

$$\frac{\overline{M} \overline{v}^2}{2} = \frac{3T}{2} \quad (5.1)$$

where \overline{M} is the average mass of the particles, \overline{v} is the average velocity and T is the temperature. The number of particles having velocity v , $n(v)$, out of the total population of plasma particles N , is given by the following equation.

$$n(v) = N \left(\frac{M}{2\pi T} \right)^{\frac{3}{2}} e^{\left(-\frac{Mv^2}{2T} \right)} \quad (5.2)$$

When plasma comes into contact with a surface, the charge carriers hit the wall and loose their charge. Electrons, having more kinetic energy, are absorbed by the wall faster. Thus a region of net positively charged plasma is formed around the surface. This is called a sheath. Sheaths are formed around spacecrafts and satellites as they coast in the exosphere of the earth. Sheaths also form on the surface of probes that are

introduced into the plasma to measure its properties.

The charged particles within the plasma exert electrostatic (Coulombic) forces on each other. Consider an electron within a plasma. Positive particles are attracted by this electron and move closer to it while negative particles are repelled by the electron and move away from it. The maximum distance within the plasma that the effect of this electron is felt is called the Debye length or Debye screening length. It is named after Peter J. W. Debye (1884-1966), a Dutch-born American physicist and 1936 Physics Nobel Prize Laureate.

The region around the electron with radius equal to its Debye length forms a Debye sphere. If a charge is present in vacuum its effect is theoretically felt into infinity. However, for a plasma, there is a huge number of charged particles in close proximity, and therefore, the charge effect can be neglected outside the Debye Length.

The Debye lengths λ_D [13] for electrons are expressed by the following equation where k is the Boltzmann's Constant, e is the charge of the electron, n_e is the concentration of the electrons and T_e is the electron temperature.

$$\lambda_D = \frac{k T_e}{4 \pi e^2 n_e} \quad (5.3)$$

Electric fields applied to a plasma can penetrate only in the order of the Debye length of the plasma, i. e. multiples of the Debye length, and this sheath thickness is proportional to the strength of the electric field applied. These concepts are important for the understanding of Langmuir probes.

5.1 Langmuir Probes

Electrical probes inserted into the plasma to study its properties were introduced by Irving Langmuir in the 1920s. Such probes are used to measure properties of the plasma, such as ion density and ion temperature, which are obtained from the probe characteristics, obtained by measuring current and probe bias voltage. There are two types of Langmuir probes used: the single probe and the double probe, as shown in figure 5.1. Their operations are similar.

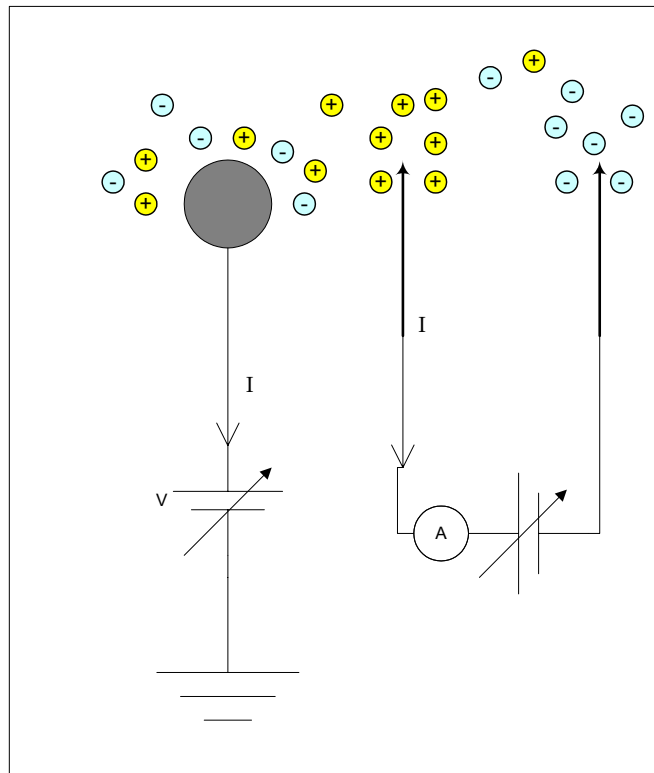


Figure 5.1: Langmuir probes, single (left) and double (right) types.

Langmuir probes consist of spherical, cylindrical or flat plate type conductors that are immersed into the plasma. The current flow due to the charges picked up and the bias voltage applied to the probe are measured by appropriate circuits.

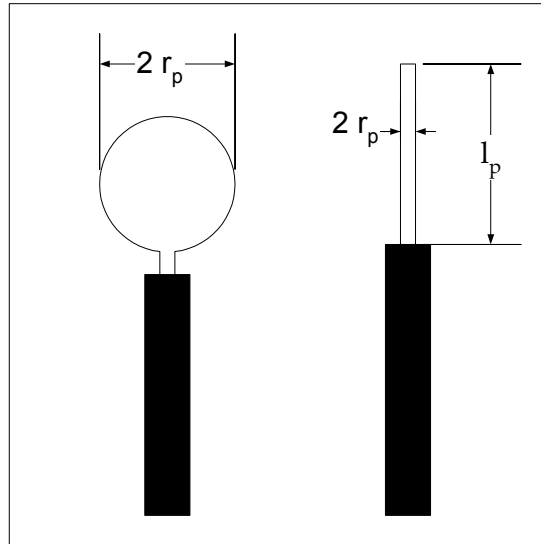


Figure 5.2: Probe characteristic lengths.

The general assumption made for studying Langmuir probe characteristics is that the plasma is composed of positive ions and electrons, i. e., there are no negatively charged particles, except electrons. When the probe is inserted into the plasma, a potential difference is created. The plasma may be at a different potential ϕ_s from the probe potential ϕ_p . As a result, a sheath is formed around the probe, whose thickness is assumed to be a multiple of the Debye length λ_D . The sheath thickness is directly proportional to the probe potential. Outside of the sheath, the plasma is undisturbed by the probe.

The probe potential is often applied in the form of a saw tooth waveform. The probe potential and the current measured are used to study the probe characteristics. Charge density and temperature can be determined from the probe characteristics. The number of charged particles may be calculated from the following equation.

$$n = \frac{4 I_{p0}}{A_p q \bar{v}} \quad (5.4)$$

I_{p0} is the probe current when probe potential is zero, A_p is the effective probe area, q is the charge of the particle and \bar{v} is the average velocity of the particle. The average velocity is given by

$$\bar{v} = \sqrt{\frac{8 k T}{\pi m}} \quad (5.5)$$

where k is Boltzmann's constant and m is the mass of the particle. The temperature of the charge particles may be obtained from the slope of the probe characteristics on a semi-logarithmic scale of the voltage as

$$T = -\frac{q}{k_B} \frac{d}{dU_p} \ln\left(\frac{I_p}{I_{p0}}\right) \quad (5.6)$$

where U_p is the applied probe potential and I_p is the probe current, I_{p0} is the probe current when $U_p = 0$.

Langmuir probes are technically simple and easy to implement. From just simple probe voltage and current measurements, many plasma properties such as charge densities and temperatures may be calculated. However, there are some drawbacks. The mass of the charge carriers needs to be known. The plasma is disturbed by the introduction of the probe and causes a draining of the charge carriers.

5.2 Probes Used in the Bench Test

The probes used for this study were very simplistic. The circuits used are shown in figures 5.3 and 5.4 below. The probes are made by inserting stainless steel needles

(sewing needles) into ceramic tubes, with a portion sticking outside. To find the surface areas of the needles that are exposed, the needles are modelled as a cone atop a cylinder. Each needle is 1 mm in diameter, and the conic section is 5 mm long. The surface areas of each of the double probe are found to be $3.29 \times 10^{-5} \text{ m}^2$ and that of the single probe is $4.87 \times 10^{-5} \text{ m}^2$.

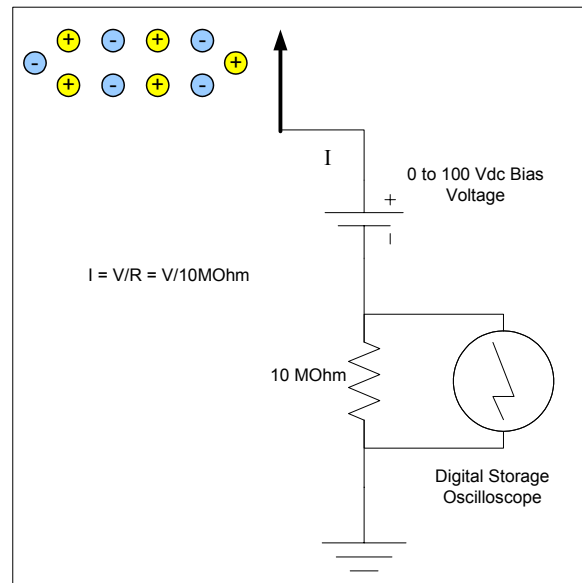


Figure 5.3: Single probe circuit.

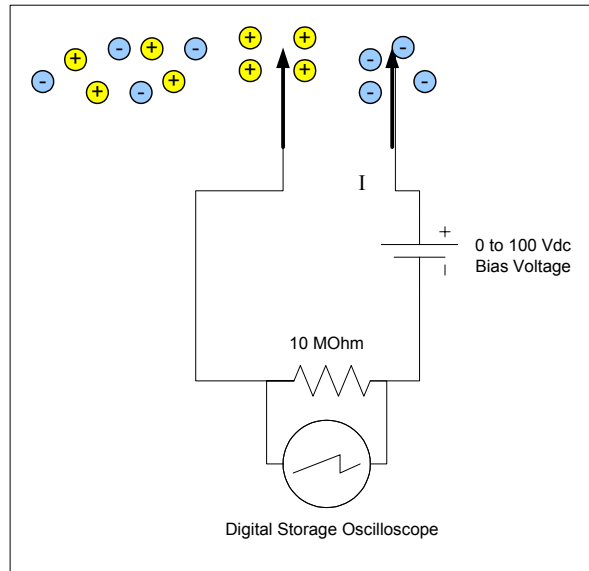


Figure 5.4: Dual probe circuit.

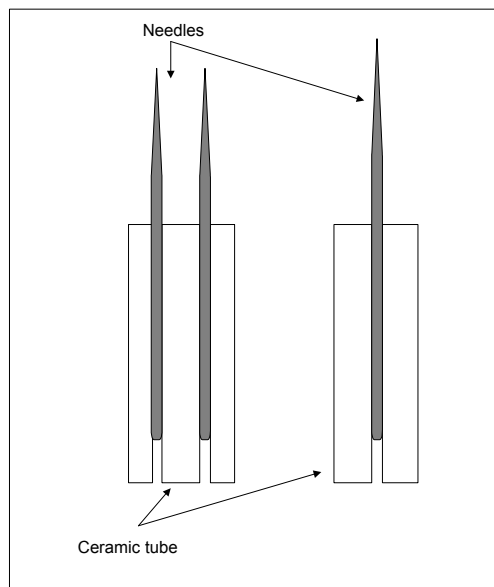


Figure 5.5: The probe needles.

With these probes, the waveform of the voltage across the resistor could be observed on an oscilloscope. The current flow is given by Ohm's law $I = V/R = V/10$ MΩ. There was no bias voltage applied for the tests.

CHAPTER VI

BENCH TESTING OF TEST SECTION IN STATIC AND SLOW SPEED AIR

6.1 Bench Test Results

The setup for the bench testing of the test section is shown below in figure 6.1. The test section is placed in ambient air and a high dc potential is applied. A blower fan is placed in front of the test section to cause the ions to flow out. The high voltage dc power is applied to the electrodes and observations of the voltage across the electrodes, the current flow from the power supply and effects due to corona discharge are noted.

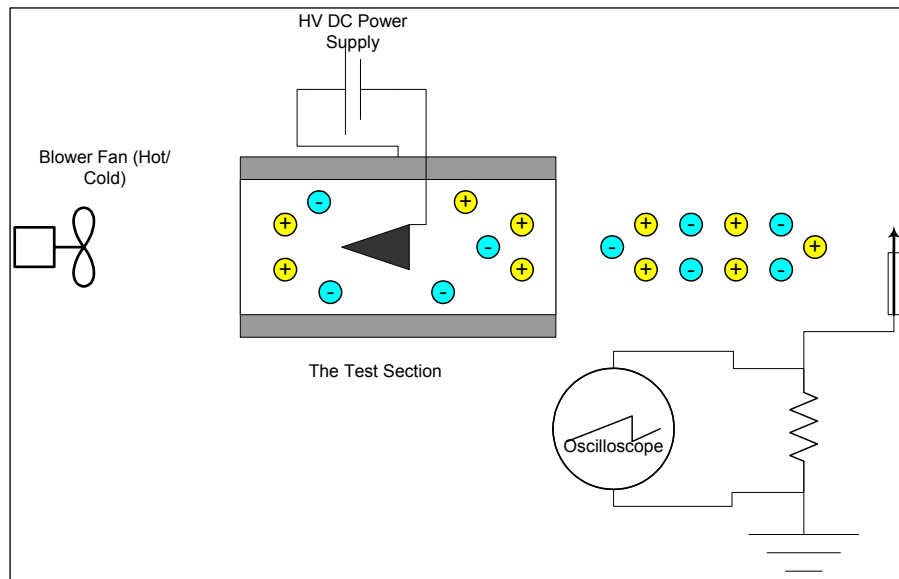


Figure 6.1: Setup for bench testing.

Table 6.1 is a qualitative record of the results of the initial bench testing. For the wedge made negative, there was no corona visible up to 9.5 kV. There was a hissing sound and smell of ozone in the air at lower voltages. At 9.5 kV, one glowing spot of

corona was visible on the knife edge of the wedge, about 5 mm from the top. As the voltage was increased, two corona spots became visible on the knife edge at 10 kV, with the new one about 5 mm from the bottom. At 11 kV, there were four corona spots visible, such that they were roughly equally spaced from each other. At a little over 11.5 kV, a loud arc shot across the wedge to the pipe. The corona is seen as bluish-white spots on the tip of the sharp edge of the wedge.

For the tests with the wedge made positive with respect to the pipe, there was strong hissing sound and smell of ozone in the air; however, there were no visible corona up till the arcing at about 10 kV. It was observed that arcing occurred at a lower voltage for positive corona. Also, there were spots of corona visible on the fixtures on the outside of the pipe, which was negative with respect to the wedge.

Table 6.1: Initial bench test results.

Negative Corona		Positive Corona	
Voltage	Effects	Voltage	Effects
9000 V	Nil	4500 V	Spot seen on outside, no corona inside
9550 V	One corona spot	6000 V	Spots of corona on outside
10000 V	Two corona spots, hissing sound	7000 V	Spots of corona on outside
10570 V	Two corona spots, hissing sound	8000 V	Spots of corona on outside
11040 V	4 corona spots, strong hissing.	9000 V	Spots of corona on outside
11555 V	Loud Arc shot once, power supply cut off	10035 V	Loud Arc, power supply cut off.

After several tests, the arcing caused the Lexan surface to char leaving a carbonized trail over the surface across which the arc had discharged. This carbon trail conducted electricity. Therefore, the test section had to be removed and cleaned.

Following the reassembly, the test section was put through further tests. Figure 6.2 shows the results for both positive and negative corona tests. A maximum ceiling voltage of 7 kV was maintained to prevent arcing. For negative corona tests, corona was visible at a lower voltage now than when the test section was new. This could be ascribed to impurities present on the wedge and inside the test section. There was no visible corona for the case where the wedge was positive.

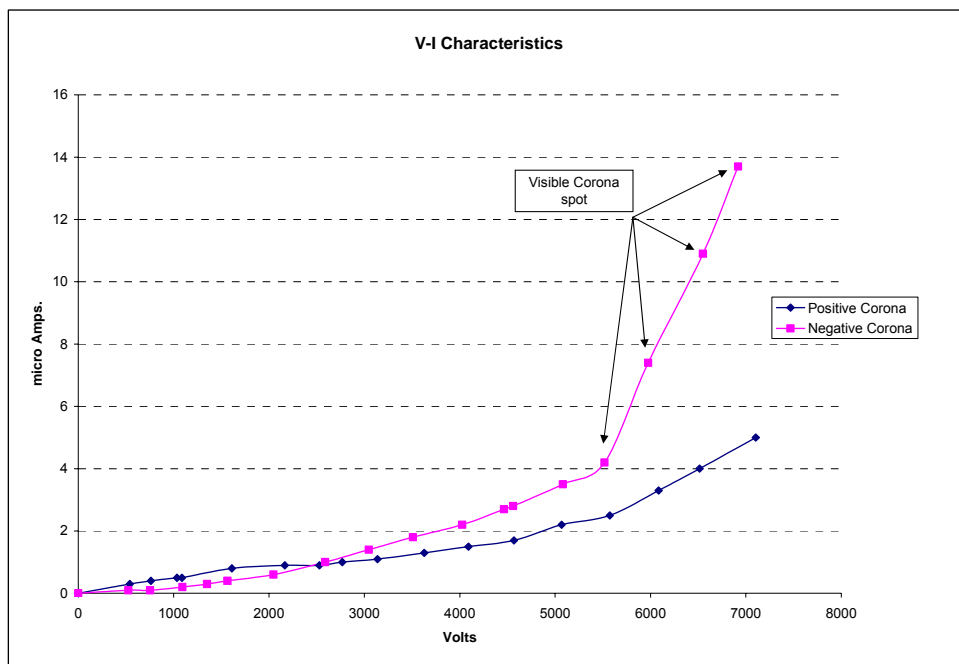


Figure 6.2: Voltage-current characteristics of corona for the test section.

Due to the deterioration of the Lexan surface caused by the arcing, several attempts were made to protect it from charring. Electrical insulating varnish was applied, but this compound has a low tolerance to high temperatures. Also the solvent present in the varnish causes damage to the Lexan. Teflon strips were glued to the surface with special adhesive for Teflon; however they became unstuck when pressure was applied. Finally, a ceramic cement called Sauereisen Electrotemp Cement No. 8 Powder [37] was

applied. It is composed of Silica (SiO_2), Zirconium Silicate (ZrSiO_4), Magnesium Oxide (MgO) and Magnesium Phosphate (MgHPO_4). It is in a powder form that is mixed with water, made into a paste and applied. It sets after half an hour and takes 24 hours to cure. Once cured it forms a strong contact and a hard surface. The setting is due to the reaction of the phosphate with water. It has high electrical resistivity, heat conductivity and resistant to thermal shocks (which can occur due to an arc). It has a dielectric strength rated at 2900 to 3900 V/mm at 21°C. It can withstand temperatures up to 1426°C.

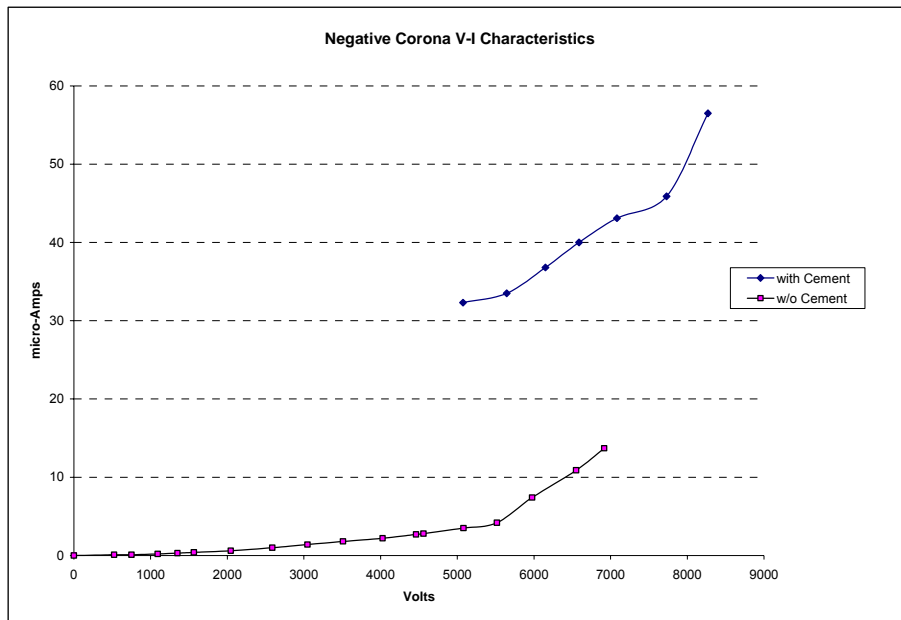


Figure 6.3: Voltage-current characteristics for negative corona before and after the application of ceramic cement.

When the test section was subjected to tests after the application of the cement, it was observed that the current flow from the power supply had increased by more than a factor of 10. This is shown in figure 6.3. The increase in current at lower voltages is credited to a phenomenon known as Malter effect. An interesting point to note here is

that when the cement was removed the V-I readings returned to the original state.

6.2: Malter Effect

Malter effect was discovered by Louis Malter [40] who documented it in a 1936 article in the Physical Review. He observed that when alumina (Al_2O_3), a non conductor and constituent of ceramic, is applied to a cathode which is stressed to a high negative potential with respect to the anode, and is subjected to electron bombardment, secondary electron emission occurs from the alumina surface. This leaves a net positive charge on the alumina surface causing it to become polarized. Since alumina is an insulator, the positive charge does not neutralize as fast as it is built up. Thus a stronger gradient occurs across the electrodes, resulting in emission of electrons from the cathode surface. This emission is seen to increase with the voltage applied.

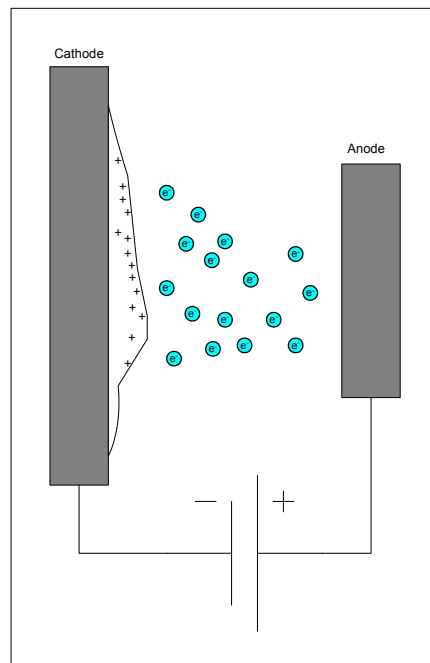


Figure 6.4: Electrons released from the surface of the insulator on the cathode due to Malter effect.

The secondary emission does not stop when the electron bombardment is removed, but gradually decays. Shining light up on the cathode was found to reduce the emission. Malter observed this effect on Al_2O_3 , MgO , Zn_2SiO_3 , SiO_2 , ZrO_2 , CaCO_3 , Ta_2O_5 and a few other oxides.

For Malter effect to occur, the following conditions must be met. The cathode must be covered partially by an insulator. There must be an initiating source for the emission, like an electron bombardment or strong ionization, such as corona discharge. The rate at which electrons are emitted must be greater than the rate of removal of the positive charge from the surface of the insulator.

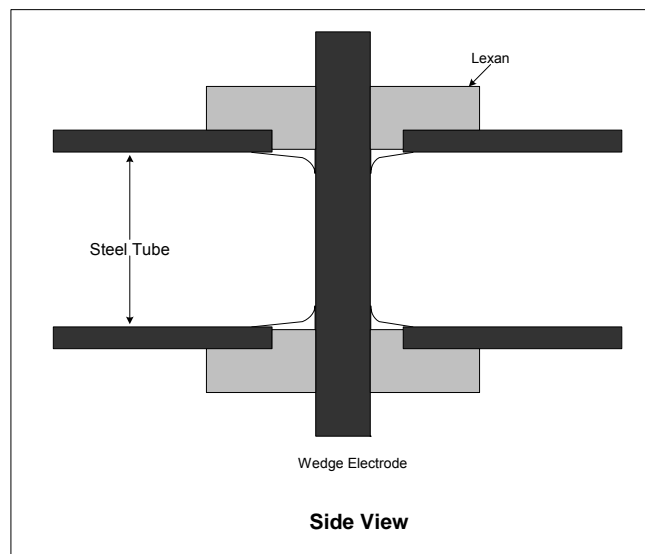


Figure 6.5: Side view of the test section showing the ceramic cement application overlapped on the wedge.

For the test section, when the ceramic cement was applied, cement was partly overlapping the wedge electrode, as shown in figure 6.5. Subsequent tests showed that corona was seen to occur at a lower voltage and the current flow was seen to be much

higher than for the clean configuration. Malter effect is suspected for this increase in current.

6.3: Results of the Ion Detector Probes

The ion detector probes yielded a complex waveform that was observed on a digitizing oscilloscope. The waveform pattern was as shown in figure 6.6. It shows a sharp peak of about 5ms duration followed by a flat plateau region. The frequency of this waveform is 60 Hz. It is thought that the probe acts like an antennae and picks up noise from the power supply. The sharp peak is due to the charging of the capacitor. This peak increases in intensity as the probe is brought closer to the test section and drops as the probe is moved away. However, it is not a conclusive evidence of ion detection. Therefore, a more sophisticated circuit involving amplifiers has to be assembled.



Figure 6.6: The waveform picked up by the ion detector probes.

A different type of probe circuit [41] is proposed to measure the current, as shown below. This circuit has a current to voltage converter amplifier or trans-impedance amplifier that can measure the extremely small currents that are picked up due to the ions.

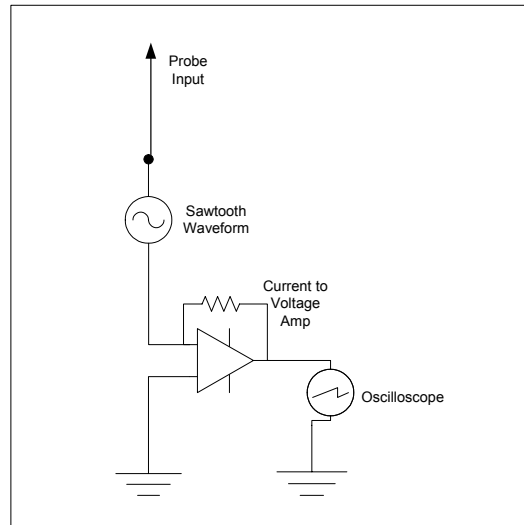


Figure 6.7: Proposed new probe circuit.

CHAPTER VII

CONCLUSIONS AND RECOMMENDATIONS

7.1 Conclusions

The High Voltage Power Supply that was built has been found to fit the requirements adequately. It is able to deliver dc voltages up to about 15 kVdc, beyond the required level for corona discharge in the test section, which is up to 8 kVdc. There is however a small drop in voltage as higher currents are drawn. This can be compensated for by raising the input voltage.

The test section has been found to be suitable for the generation of corona. Corona was observed for both positive and negative polarity. However, at higher voltages, initially greater than 11 kV for negative corona and 10 kV for positive corona, strong arcing was observed. Arcing was prevented by the introduction of current limiting resistors. Yet despite the resistors, high current corona streamers were observed at high voltages of about 9 kV that charred the surface of the Lexan. These streamers were found to originate at the rear of the wedge, where it is closest to the steel pipe. This caused carbonization of the surface leading to conduction. The streamers seemed to be erratic, sometimes originating at mid level voltages about 8 kV. Several methods were tried to treat the Lexan surface. Electrical insulating varnish caused slight erosion of the surface but offered no protection from charring. A thin coating of ceramic cement on the surface was found to be mechanically strong. However, the threshold of corona

was now found to be lowered, with corona spots being visible at as low as 4 kV. Current flows were considerable higher, i.e., where the current at 5 kV were earlier found to be immeasurable ($< 1 \mu\text{A}$), now it seemed to be in the range of 35 to 40 μA . This is thought to be an indication of the Malter effect.

The probes built for the tests detected the presence of ionic charges in the area outside the charged test section and show a drop in intensity of waveform as distance from the test section was increased. However, the results were inconclusive and the circuit is thought to be not sophisticated enough to determine ion density and temperature. This is because the circuit contains only passive devices, resistors and capacitors, with no amplifiers, and therefore, the current flow due to ions is not strong enough to be quantified. Still, the waveform does show presence of ions.

7.2 Recommendations

A different step-up high-voltage transformer, with better secondary regulation, would render improved regulation to the High Voltage DC Power Supply. Neon transformers inherently have poor regulation as they are designed for neon light applications where such performance is required. Such a powerful step up transformer with high secondary ratings would be expensive. A flatter dc output would be obtained if the size of the filter capacitor is increased. Although 1 μF performs quite well, a higher rated capacitor would further reduce the ripples. It is recommendable to purchase another high voltage power relay to cut off the 500 M Ω voltage divider resistors from the capacitor to prevent draining the capacitor when pure dc is required from the capacitor with the ac power turned off.

The biggest set back faced with the test section is the Lexan insulator blocks getting charred by the arcing. It would be better to build the test section with ceramic insulation instead because ceramic has better mechanical strength, can withstand higher temperatures, has a higher dielectric strength and is resistant to solvents [38].

The probe circuit has to be modified to include a current to voltage converter or a trans-impedance amplifier. This can enable the measurement of feeble currents that are created by the ions.

More tests need to be carried out to determine if the Malter effect is indeed the reason behind the lowering of the corona threshold voltage and to uncover the effects on the test section. If Malter effect is occurring, it would be advantageous to have a lower corona threshold in a supersonic combustion engine application [39].

AC of high frequency (>100 kHz) is recommended for increased ionization especially at high pressures. The starting voltage for the onset of corona increases as pressure and electrode spacing goes up. With DC corona, a sheath is formed around the electrodes. This would not be the case for supersonic flow corona, as the plasma would get dislodged and carried away by the flow. As the frequencies are increased, the sheath region also changes in size and the ions cross the sheaths rapidly. Thus the ions gain kinetic energies and two effects are observed. Firstly, it results in increased secondary ionization away from the electrodes, and secondly, there is ionic heating of the plasma due to the displacement current. Thus, less voltage levels are required for AC corona. For industrial applications, plasma is generated using high frequencies in the MHz range. Power supplies for plasma generation are available commonly at 13.56 MHz.

APPENDIX A

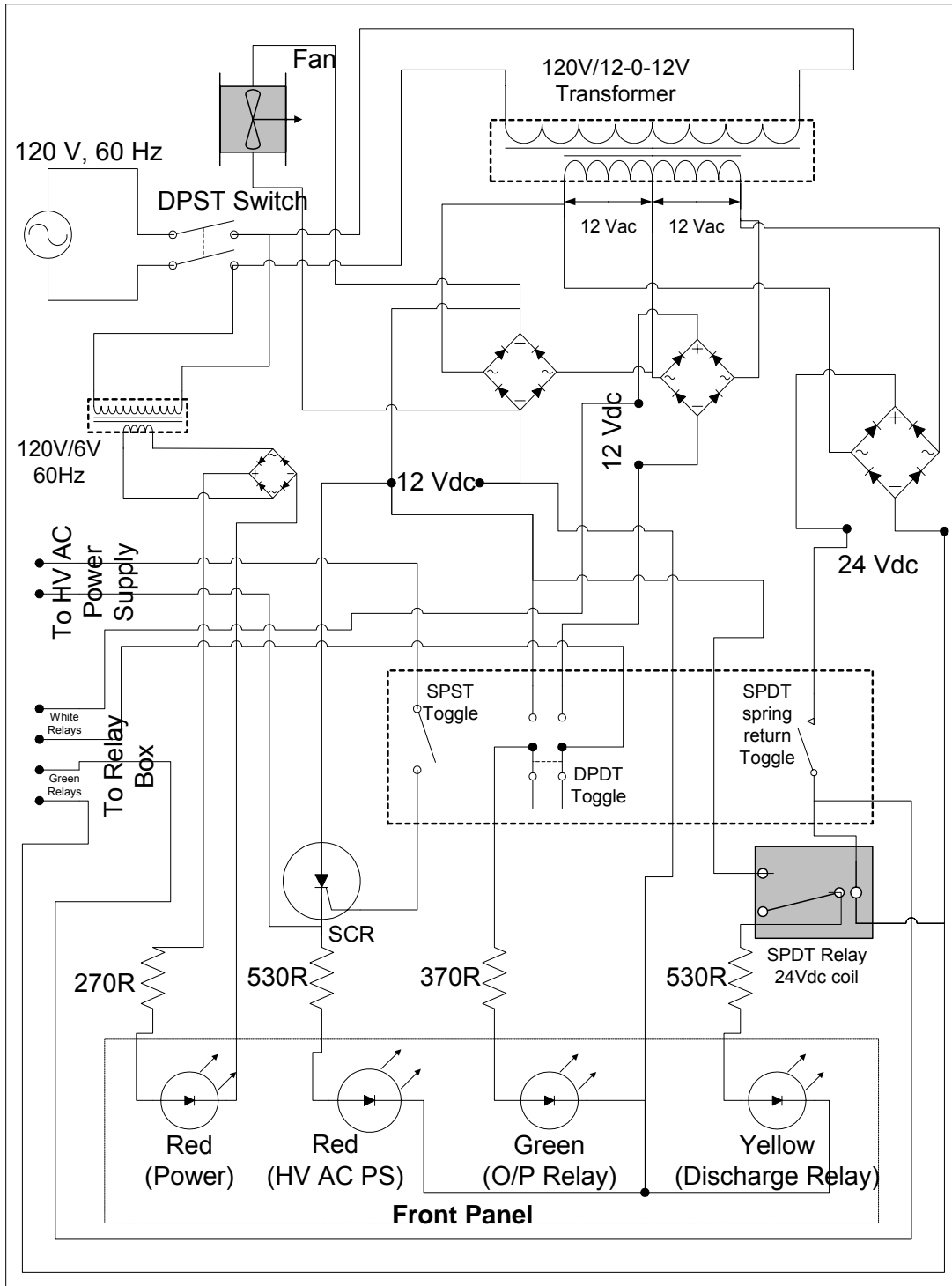
CIRCUIT DIAGRAM OF THE HIGH VOLTAGE AC GENERATOR

APPENDIX B

CIRCUIT DIAGRAM OF THE HV DC POWER SUPPLY

APPENDIX C

CIRCUIT DIAGRAM OF THE CONTROL BOX



REFERENCES

1. Keidar, M., Boyd, I. D., Beilis, I. I., "Plasma Flow and Plasma-Wall Transition in Hall Thruster Channel", *Physics of Plasmas*, Vol. 8, No. 12, Dec. 2001.
2. Artana, G., D'Adamo, J., Leger, L., Moreau, E., Touchard, G., "Flow Control with Electrohydrodynamic Actuators", *AIAA Journal*, Vol. 40, No. 9, Sep. 2002.
3. Yano, R., Contini, V., Plonjes, E., Palm, P., Merriman, S., Aithal, S., Adamovich, I., Lempert, W., Subramaniam, V., Rich, J. W., "Supersonic Nonequilibrium Plasma Wind-Tunnel Measurements of Shock Modification and Flow Visualization", *AIAA Journal*, Vol. 38, No. 10, Oct. 2000.
4. Stuessy, W. S., Murtugudde, R. G., Lu, F. K., Wilson, D. R., "Development of the UTA Hypersonic Shock Tunnel", *AIAA Paper 90-0090*, 1990.
5. Stuessy, W. S., Liu, H. C., Lu, F. K., Wilson, D. R., "Experiments on Weakly Ionized Air and Nitrogen Plasmas for Hypersonic Propulsion Facility Development", *AIAA Paper 99-2448*, 1999.
6. Liu, H. C., "Electrical Conductivity Measurement of a High Pressure Seeded Air Plasma", Ph.D. Dissertation U.T.A., 1998.
7. Tishkoff, J. M., Drummond, J. P., Edwards, T., Nejad, A. S., "Future Directions of Supersonic Combustion Research: Air Force/ NASA Workshop on Supersonic Combustion", Newport News, Virginia, 1996.
<http://techreports.larc.nasa.gov/ltrs/PDF/1997/aiaa/NASA-aiaa-97-1017.pdf>
8. www.geplastics.com
9. <http://www.colorado.edu/physics/2000/bec/>

10. <http://www.bec.nist.gov/>
11. <http://www.ee.nmt.edu/~langmuir/langmuir.html>
12. http://fusedweb.ppppl.gov/CPEP/Chart_Pages/5.Plasma4StateMatter.html
13. Hippler, R., Pfau, S., Schmidt, M., Schoenbach, K. H., *Low Temperature Plasma Physics: Fundamental Aspects and Applications*, Wiley-VCH, NY, 2000.
14. Smirnov, B. M., *Introduction to Plasma Physics*, Mir Publishers, Moscow, 1977.
15. The National Research Council, *Plasma Science: From Fundamental Research to Technological Applications*, National Academy Press, Washington, D.C., 1995.
16. Wilson, R.G., Brewer, G. R., *Ion Beams: With Applications to Ion Implantation*, Robert E. Krieger Publishing Company, Huntington, NY, 1973.
17. Loeb, L., B., *Electrical Coronas: Their Basic Physical Mechanisms*, University of California Press, Berkeley, 1965.
18. Anikin, N. B., Pancheshnyi, S. V., Starikovskaia, S. M., Starikovskii, A. Y., “Air Plasma Production by High Voltage Nanosecond Gas Discharge”, AIAA 2001-3088.
19. Aleksandrov, N. L., Anikin, N. B., Bazelyan, E. M., Zatsepin, D. V., Starikovskaia, S. M., Starikovskii, A., Y., “Chemical Reactions and Ignition Initiation in Hydrocarbon-Air Mixtures by High Voltage Nanosecond Gas Discharge”, AIAA 2001-2949.
20. Shale, C. C., Bowie, W. S., Holden, J. H., Strimbeck, G. R., “Characteristics of Positive Corona for Electrical Precipitation at High Temperatures and Pressures”, United States Department of the Interior, Bureau of Mines, 1964.

21. <http://pulsedpower.usc.edu/>
22. Vinogradov, J., Sher, E., Rutkevich, I., Mond, M., “Voltage-Current Characteristics of a Flame-Assisted Uni-polar Corona”, Pearlstone Center for Aeronautical Studies, Dept. of Mechanical Engg., Ben-Gurion University of the Negev, Beer Sheva, 84105 Israel, 2001.
23. Chernikov, V. Ershov, A., Shibkov, V., Timofeev, I., Timofeev, B., Vinogradov, V., Van Wie, D., “Gas Discharges in Supersonic Flows of Air-Propane Mixture”, Moscow State University, Moscow, Russia, 2001.
24. Ekchian, J., Nowak, V., Rush, J., “A Compact Corona Discharge Device (CCD) for Non –Thermal Plasma Generation in Gasoline or Diesel Engine Exhaust”, Litex, Inc., <http://www.osti.gov/hvt/deer2000/deer2000wkshp.html>
25. Jackson, S., P., *Selection and Application of Metallic Rectifiers*, McGraw-Hill, NY, 1957.
26. <http://science.howstuffworks.com>
27. Rashid, M., H., *Power Electronics, Circuits, Devices and Applications*, 2nd Edition, Prentice-Hall International, New Delhi, India, 1996.
28. http://www.repairfaq.org/REPAIR/F_flytest.html
29. <http://www.hills2.u-net.com/tesla/neon.htm> [used with permission from Christopher J. Hill, cjhill@hills.u-net.com]
30. <http://www.franceformer.com>
31. Cheng, D., K., *Field and Wave Electromagnetics*, 2nd Edition, Addison-Wesley Publishing Company, NY, 1989.
32. Asokan, T., “Ceramic Dielectrics for Space Applications”, *Current Science*, Vol. 79, No.3, 10 August 2000.

- <http://tejas.serc.iisc.ernet.in/~currsci/aug102000/mg7.pdf> [used with permission from the author]
33. <http://www.jenningstech.com>
 34. <http://www.kilovac.com>
 35. Holman, J. P.: *Experimental Methods for Engineers*, 7th ed., McGraw Hill, New York, 2001
 36. <http://www.blpcomp.com/productinfo/filters2.php>
 37. <http://www.sauereisen.com/index.htm>
 38. <http://matse1.mse.uiuc.edu/~tw/ceramics/ceramics.html>
 39. <http://www.yet2.com/app/insight/tehofweek/25253?sid=200>
 40. Malter, L., "Thin Film Field Emission", *Phys. Rev.* 49, 478, Vol. 50, July 1936.
 41. Batani, D., Alba, S., Lombardi, P., Galassi, A., "Use of Langmuir Probes in a Weakly Ionized, Steady-State Plasma With Strong Magnetic Field", *Rev. Sci. Instrum.* 68 (11), November 1997.

BIOGRAPHICAL INFORMATION

Philip Panicker was born on the 4th of September 1973 in the small town of Mavelikara, in the southern most state of India called Kerala. He attended The Bishop Moore Vidhyapith School in Mavelikara up to the 3rd standard and The Indian High School Dubai, Dubai, United Arab Emirates, till the 12th standard. He completed the Bachelor of Engineering in Electronics and Telecommunication degree in 1995 at M. S. Ramaiah Institute of Technology, Bangalore, India. In 1999 he was accepted to the college of Mechanical and Aerospace Engineering of The University of Texas at Arlington (UTA). For two years he had to undertake prerequisite subjects for the change of major from Electronics to Aerospace Engineering. In the fall of 2001, he joined the research team of Drs. Frank Lu, Don Wilson, George Emanuel and Bernard Svihel at the Aerodynamics Research Centre (ARC) of the UTA to pursue research in experimental high speed gas dynamics and propulsion.

He has plans to obtain a PhD and continue research in several areas of interest, including experimental gas dynamics, propulsion, power generation and the exploration of renewable sources of energy generation. He has been a student member of the American Institute of Aeronautics and Astronautics since the year 2000. This is a detailed report of his work done for the Masters of Science in Aerospace Engineering degree presented in August 2003.